

AD-A062 659

UNIVERSAL ENERGY SYSTEMS INC DAYTON OHIO
LARGE VOLUME PLASMA PRODUCTION BY 2.45GHZ MICROWAVES.(U)
DEC 77 R DARRAH

F/G 20/9

UNCLASSIFIED

AFAPL-TR-77-85

F33615-75-C-1082

NL

1 OF 2
ADA
082659



A
65

AD A062659

DDC FILE COPY

AFAPL-TR-77-85

②
NW

LEVEL II

**LARGE VOLUME PLASMA PRODUCTION
BY 2.45 GHZ MICROWAVES**

UNIVERSAL ENERGY SYSTEMS, INC.
RODNEY DARRAH
3195 PLAINFIELD ROAD
DAYTON, OHIO 45432

DECEMBER 1977

TECHNICAL REPORT AFAPL-TR-77-85
Final Report - 9 December 1974 - 16 May 1977

DDC
RECEIVED
DEC 29 1978
B

Approved for public release; distribution unlimited.

AIR FORCE WRIGHT AERONAUTICAL LABORATORIES
AIR FORCE SYSTEMS COMMAND
AIR FORCE AERO PROPULSION LABORATORY
WRIGHT-PATTERSON AIR FORCE BASE, OHIO 45433

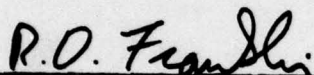
78 12 26 001

NOTICE

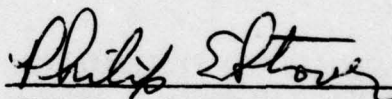
When Government drawings, specifications, or other data are used for any purpose other than in connection with a definitely related Government procurement operation, the United States Government thereby incurs no responsibility nor any obligation whatsoever; and the fact that the government may have formulated, furnished, or in any way supplied the said drawings, specifications, or other data, is not to be regarded by implication or otherwise as in any manner licensing the holder or any other person or corporation, or conveying any rights or permission to manufacture, use, or sell any patented invention that may in any way be related thereto.

This report has been reviewed by the Information Office (OI) and is releasable to the National Technical Information Service (NTIS). At NTIS, it will be available to the general public, including foreign nations.

This technical report has been reviewed and is approved for publication.

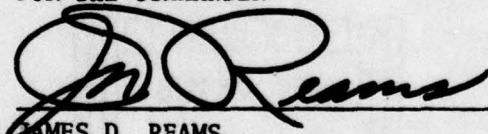


RICHARD D. FRANKLIN, Capt, USAF
Project Engineer



PHILIP E. STOVER
Chief, High Power Branch

FOR THE COMMANDER



JAMES D. REAMS
Chief, Aerospace Power Division

"If your address has changed, if you wish to be removed from our mailing list, or if the addressee is no longer employed by your organization please notify AFAPL/POD-2, W-PAFB, OH 45433 to help us maintain a current mailing list".

Copies of this report should not be returned unless return is required by security considerations, contractual obligations, or notice on a specific document.

19 REPORT DOCUMENTATION PAGE		READ INSTRUCTIONS BEFORE COMPLETING FORM
1. REPORT NUMBER 18 AFAPL TR-77-85	2. GOVT ACCESSION NO.	3. RECIPIENT'S CATALOG NUMBER
4. TITLE (and Subtitle) 6 LARGE VOLUME PLASMA PRODUCTION BY 2.45GHz MICROWAVES.	5. TYPE OF REPORT & PERIOD COVERED 9 Final Report 9 Dec 74 - 16 May 77	6. PERFORMING ORG. REPORT NUMBER
7. AUTHOR(s) 10 Rodney/Darrah	8. CONTRACT OR GRANT NUMBER(s) 15 F33615-75-C-1082 new	9. PROGRAM ELEMENT, PROJECT, TASK AREA & WORK UNIT NUMBERS 16 2301-52-78 17 52
10. PERFORMING ORGANIZATION NAME AND ADDRESS Universal Energy Systems, Inc. 3195 Plainfield Road Dayton, Ohio 45432	11. CONTROLLING OFFICE NAME AND ADDRESS Air Force Aero Propulsion Laboratory (POD) Air Force Systems Command Wright-Patterson AF Base, Ohio 45433	12. REPORT DATE 11 December 1977
13. MONITORING AGENCY NAME & ADDRESS (if different from Controlling Office) 12 96p.	14. SECURITY CLASS. (of this report) Unclassified	15. DECLASSIFICATION/DOWNGRADING SCHEDULE
16. DISTRIBUTION STATEMENT (of this Report) Approved for public release; distribution unlimited		
17. DISTRIBUTION STATEMENT (of the abstract entered in Block 20, if different from Report) DDC RECEIVED DEC 29 1978 RECEIVED B		
18. SUPPLEMENTARY NOTES		
19. KEY WORDS (Continue on reverse side if necessary and identify by block number) Microwave, Helium Electron Density, Argon Electron Density, Oxygen Singlet Delta, Oxygen Atom, He-Ne Laser, Mercury, Pulsed UV.		
20. ABSTRACT (Continue on reverse side if necessary and identify by block number) The ionization and excitation of gases by three different geometries of microwave applicators are investigated. Current-voltage characteristics of a plasma with super-imposed ionization by a 2.45 GHz applicator with transport from a dc field are measured. Electron densities in helium and argon test gases were found to be greater than 10^{12} /cc or thirty times higher than normal plasma cut-off densities. This applicator is also used to determine the percentage of O_2^+ produced in a pure oxygen microwave discharge. A production of up to 25% at low pressures is measured.		

DD FORM 1 JAN 73 1473 EDITION OF 1 NOV 65 IS OBSOLETE

390 743

1 del(g)

78

TO the 12th power

12

26

051

Jhu

SECURITY CLASSIFICATION OF THIS PAGE (When Data Entered)

A design which specially couples two applicators was implemented resulting in twice the power density and better uniformity. Measurement of the percentage of atomic oxygen produced in an oxygen discharge, determined by NO_2 titration, indicates the efficiency of atom production for this system is as high as 43 eV/atom. Microwave power is superimposed on a dc discharge in a quartz tube He-Ne laser in this system.

A twin antenna irradiator is used to apply 2.45 GHz pulsed and cw microwave power to a quartz discharge tube containing condensed mercury. The time resolved spectra of pulsed operation shows that the relative intensity of the pulsed ultraviolet output decreases as the microwave sustainer power and thus the pressure is increased.

FOREWORD

This report describes research performed by Universal Energy Systems, Inc., Dayton, Ohio. The work was conducted under Contract F33615-75-C-1082, "Investigations of Methods of Plasma Excitation", Task II, "Microwave Excitation".

The work reported herein was performed during the period 9 December 1974 to 16 May 1977 at the in-house facilities of the High Power Branch (POD-2 Bldg. 450), Aerospace Power Division (PO), Air Force Aero Propulsion Laboratory, Air Force Wright Aeronautical Laboratories, Wright-Patterson Air Force Base, Ohio. The work was conducted by the author, Mr. Rodney Darrah, Research Physicist. The report was released by the author in June 1977.

ACCESSION FOR	
NTIS	White Section <input checked="" type="checkbox"/>
DOC	Buff Section <input type="checkbox"/>
UNANNOUNCED	<input type="checkbox"/>
JUSTIFICATION	
BY	
DISTRIBUTION/AVAILABILITY CODES	
Dist. STATE only or SPECIAL	
A	

TABLE OF CONTENTS

SECTION	PAGE
I INTRODUCTION -----	1
1. Interdigital Applicator System -----	1
2. Sandwich Applicator System -----	2
3. Twin Antenna Irradiator System -----	2
II INTERDIGITAL APPLICATOR SYSTEM -----	3
1. System Description -----	3
2. Electron Density Measurements -----	12
3. Oxygen Singlet Delta Measurements -----	26
III SANDWICH APPLICATOR SYSTEM -----	35
1. System Description -----	35
2. Oxygen Atom Production -----	35
3. He-Ne Laser -----	49
IV TWIN ANTENNA IRRADIATOR SYSTEM -----	59
1. System Description -----	59
2. Pulse Ultraviolet Measurements -----	63
APPENDIX A -----	77
APPENDIX B -----	81
REFERENCES -----	83

LIST OF ILLUSTRATIONS

FIGURE		PAGE
1	Gerling-Moore 2.45 GHz - 2.5 KWatt Microwave System -----	4
2	Interdigital Slow Wave Applicator -----	6
3	Strapped-Bar Structure -----	7
4	Relative Electric Field Versus Height Above the Applicator Surface -----	8
5	Applicator Microwave Power Absorbed In A Helium Plasma Versus Pressure -----	10
6	Height Adjustment of Flow Tube Above Applicator -----	11
7	Transverse Flow Positions -----	13
8	Flow Tube and Electrode Assembly -----	14
9	Instrumentation For I-V Characteristics of He and Ar -----	16
10	Instrumentation For I-V Characteristics of He and Ar In A Pulsed Discharge -----	20
11	Helium I-V Characteristics Curve -----	23
12	Argon I-V Characteristics Curve -----	25
13	Electron Density In Helium As A Function of Pressure For Several Microwave Powers -----	27
14	Microwave Discharge System For The Production of $O_2^1\Delta g$ -----	29
15	System Used For Disposition of HgO On A Quartz Tube -----	30
16	% Yield of $O_2^1\Delta g$ As A Function of Microwave Power -----	32
17	Relative % Yield of $O_2^1\Delta g$ As A Function of Microwave Power -----	33
18	Sandwich Applicator -----	36
19	Sandwich Applicator System -----	38

LIST OF ILLUSTRATIONS (Continued)

FIGURE		PAGE
20	Oxygen Flow System -----	40
21	NO ₂ Titration System -----	42
22	Log K Versus 1/T for NO ₂ System -----	46
23	Percent of Oxygen Atom Production Versus Microwave Power -----	50
24	Quartz Tube He-Ne Laser -----	53
25	Instrumentation For The Measurement of the Laser Beam Optical Output Power -----	55
26	Laser Beam Optical Power Output Change With Respect to Absorbed Microwave Power -----	57
27	Twin Antenna Irradiator System -----	61
28	Instrumentation For CW-UV Spectral Measurements -----	61
29	Mercury Spectrum of 930W CW Discharge -----	64
30	Instrumentation For Pulsed Microwave Application to the Twin Antenna Irradiator -----	65
31	Instrumentation for Pulsed UV -----	69
32	Relative Instrument Sensitivity Factor As A Function of Wavelength -----	72
33	Mercury Spectrum From 200 Watt Discharge In Lossy Coaxial Mode -----	73
34	Mercury Spectrum From 100 Watt Discharge In Conductive Coaxial Mode -----	74
35	The Relative Spectral Intensity of the 220 nm to 350 nm Radiation As A Function of Microwave Power for Two Modes of Tube Operation -----	75

LIST OF TABLES

TABLE		PAGE
1.	The Accuracy of the Variables Used For The NO ₂ Flow Calculation Was Estimated and the Corresponding Error in the Flow Measurement is Shown for the Flow Range Discussed. -----	48
2	A Comparison of the Oxygen Atom Production Efficiency for Various Methods of Microwave Excitation Is Shown. -----	51
3	Data on the Change in a DC Operated He-Ne Laser's Power Output as Microwave Energy is Absorbed in the Lasing Medium Is Listed. -----	56
4	A Comparison of the UV Output From a Mercury Discharge When Operated CW and Pulsed. -----	67

SUMMARY

A large volume Gerling-Moore microwave applicator is utilized for plasma production. The applicator is a plane surface, interdigital structure with a 46 cm by 4 cm active surface. A 1.1 cm i.d. quartz tube with nickel dc electrodes is placed above and parallel to the long surface dimension. The gas, at fractional atmospheric pressures, flows through this tube and is ionized by the 2.45 GHz evanescent wave above the applicator. By raising the tube a few millimeters above the surface at the input power end of the applicator, the microwave power is absorbed along the entire length of the tube. The resulting plasma is homogeneous along the tube, except for structure on the order of the interdigital spacings. A dc electric field is applied along the axis of the tube with values below those required to sustain a dc discharge. Varying the microwave power gives an independent control of plasma parameters without being constrained to the usual relations found between the similarity parameters of the purely dc discharge. The current-voltage characteristics are measured to determine the electron density in the plasma. In helium the electron density is on the order of $1.2 \times 10^{12}/\text{cc}$, and in argon the electron density is on the order of $2.6 \times 10^{12}/\text{cc}$.

An electrodeless tube is also used in this system to obtain O_2 a¹Δg production in an oxygen discharge. High purity oxygen is used. The quartz tube has an HgO ring deposited on it to eliminate the atomic oxygen species which deplete the O_2 a¹Δg. A maximum yield of O_2 a¹Δg

of 25% at low pressure is obtained. The intensity of the 634 nm radiation of a colliding pair is measured as a function of applied microwave power. The peak in the intensity of the radiation occurs at about 100 to 120 watts of microwave power.

A sandwich of two interdigital applicators is used to obtain a more homogeneous discharge, eliminating the structure seen at the interdigital spacings. The applicators are mounted in a shielding box which allows flow tubes to be inserted along the applicators' active surface. An electrodeless quartz flow tube is used to obtain oxygen atom production from a high purity oxygen plasma. Determination of the percent of atom production in the discharge is accomplished by the titration of NO_2 into the afterglow. Measurement of the NO_2 flow needed to quench the green fluorescence produced by the reaction of atomic oxygen with the NO_2 is accomplished by using a tapered, variable area flowmeter and controlling the temperature of the NO_2 to within $\pm 2^\circ\text{C}$. The maximum efficiency of oxygen atom production for this system is 43 eV/atom.

A quartz tube He-Ne laser is tested in the sandwich applicator system. The laser tube is a 28 cm long, 6 cm o.d., 2 mm bore quartz tube, with internal mirrors and electrodes for dc operation, filled to 1.9 torr of a mix of 87.5% He_4 to 12.5% Ne_{20} . With about 18 cm of the laser tube resting across the applicators' active surface, a discharge at 140 watts produces 0.09 mW of laser optical power output. With the laser operating with a dc discharge current controlled at 5 mA, the optical power output is 1.75 mW. As microwave power is super-imposed on this discharge, the laser output increases to 1.88 mW at about 160

watts of microwave power, but as the microwave power is increased above this level, the optical output decreases rapidly, finally quenching the lasing.

A twin antenna irradiator is used to apply 2.45 GHz microwave power to a sealed quartz discharge tube that contains an excess of condensed mercury in 7 torr of argon. The irradiator in its commercial form deposits 120 watts per centimeter along a 25 cm, 8 mm i.d. tube. When operated cw at 3000 watts the ultraviolet production efficiency is somewhat better than 20%. The mercury discharge has two modes of operation. Both appear to be coaxial with the mercury tube forming the center conductor element of the coax. The normal mode of operation is a lossy coaxial mode with the mercury discharge absorbing the microwave power with an e-folding length of about half the cavity length. Pulsed microwave power tests are also done with this system. A cw microwave sustainer is used to maintain pressures where the plasma absorption of microwave power is efficient. The time resolved spectra in pulsed operation shows that the relative intensity of the pulsed ultraviolet output decreases as the sustainer power increases, which is probably due to resonance trapping in mercury since the radiation is not emitted in a pulse length similar to the microwave pulse, but rather is emitted over a relatively long time period.

of 25% at low pressure is obtained. The intensity of the 634 nm radiation of a colliding pair is measured as a function of applied microwave power. The peak in the intensity of the radiation occurs at about 100 to 120 watts of microwave power.

A sandwich of two interdigital applicators is used to obtain a more homogeneous discharge, eliminating the structure seen at the interdigital spacings. The applicators are mounted in a shielding box which allows flow tubes to be inserted along the applicators' active surface. An electrodeless quartz flow tube is used to obtain oxygen atom production from a high purity oxygen plasma. Determination of the percent of atom production in the discharge is accomplished by the titration of NO_2 into the afterglow. Measurement of the NO_2 flow needed to quench the green fluorescence produced by the reaction of atomic oxygen with the NO_2 is accomplished by using a tapered, variable area flowmeter and controlling the temperature of the NO_2 to within $\pm 2^\circ\text{C}$. The maximum efficiency of oxygen atom production for this system is 43 eV/atom.

A quartz tube He-Ne laser is tested in the sandwich applicator system. The laser tube is a 28 cm long, 6 cm o.d., 2 mm bore quartz tube, with internal mirrors and electrodes for dc operation, filled to 1.9 torr of a mix of 87.5% He_4 to 12.5% Ne_{20} . With about 18 cm of the laser tube resting across the applicators' active surface, a discharge at 140 watts produces 0.09 mW of laser optical power output. With the laser operating with a dc discharge current controlled at 5 mA, the optical power output is 1.75 mW. As microwave power is super-imposed on this discharge, the laser output increases to 1.88 mW at about 160

SECTION I

INTRODUCTION

For the purpose of producing an excited plasma, the use of microwave power shows great promise because it is not only possible to control the spectral emission of a microwave produced plasma, but also, the electron temperature over a broad range.¹ To obtain a desired set of optimum conditions in a plasma, the characterization of the physical and chemical processes occurring in the discharge is necessary. The knowledge of these processes allows the plasma to be tailored to predictable results. The characterization of the parameters involved in a discharge requires that impurities in the plasma be kept to a minimum. The internal electrode structure needed for conventional plasma production is not required for a plasma produced by microwave energy. This feature gives the advantage of eliminating the electrodes as one source of impurities. Until recently, a critical limitation on the production of a plasma by microwave energy was that the plasma volumes were limited to a few tens of cubic centimeters with cavity resonators. Now however, large volume microwave applicators are available.²

Large volume plasma production from microwave energy was tested using three microwave applicator systems.

1. INTERDIGITAL APPLICATOR SYSTEM

A slow wave structure interdigital line applicator was used to test plasma production in helium, argon, and oxygen. Electron density measurements were made in the helium and argon plasmas from the current-voltage characteristics obtained by superimposing a dc field

on the microwave produced plasma. The production of $O_2\ a^1\Delta_g$ species in an oxygen discharge was measured by monitoring the intensity of the 634 nm radiation emission of a colliding pair.

2. SANDWICH APPLICATOR SYSTEM

Two slow wave structure interdigital line applicators were used with one placed on top of the other to form a sandwich for the discharge tube giving a more uniform microwave field than is obtained with a single applicator. This was used to test for the production of atomic oxygen in an oxygen discharge and for lasing of a He-Ne gas mixture.

3. TWIN ANTENNA IRRADIATOR SYSTEM

A twin antenna irradiator was used to apply microwave energy to a sealed mercury tube. The discharge was operated in both a cw and pulsed mode. The ultraviolet radiation resulting from the discharge was measured as a function of microwave power.

SECTION II

INTERDIGITAL APPLICATOR SYSTEM

1. SYSTEM DESCRIPTION

The experimental work with this system resulted in a paper, which was presented to the IEEE International Conference on Plasma Science at Ann Arbor, Michigan, on May 15, 1975. The paper, "Discharge Characteristics of a Plasma with Superimposed Ionization by a Slow Wave 2.45 GHz Applicator and Transport From a dc Field", by A. Garscadden, P. Bletzinger, M. Andrews, and R. Darrah described experimental techniques and discussed the results of the experiments.

Figure 1 shows the plasma microwave source, which consists of the slow wave structure meander interdigital line as a convenient large volume applicator for plasma production. The system power source consists of a 2.45 GHz 2.5 kilowatt power supply, and in addition, a microwave oven tube which is operated with a dc voltage to avoid the ripple associated with the 2.5 kilowatt supply and to provide power from 0 to 600 watts. An isolator is required in the system to protect the magnetron from reflected power above 100 watts. Although under normal use of the plasma source, even during breakdown, the reflected power is negligible, the protection is required in case of breakage in the plasma system. Power meters to monitor the incident, reflected and transmitted power associated with the applicator are calorimetrically calibrated to 3%. The direct output across the meter gives an estimate of the microwave power ripple when the non-linearities of the crystal detectors are taken into account. The applicator itself is shown open

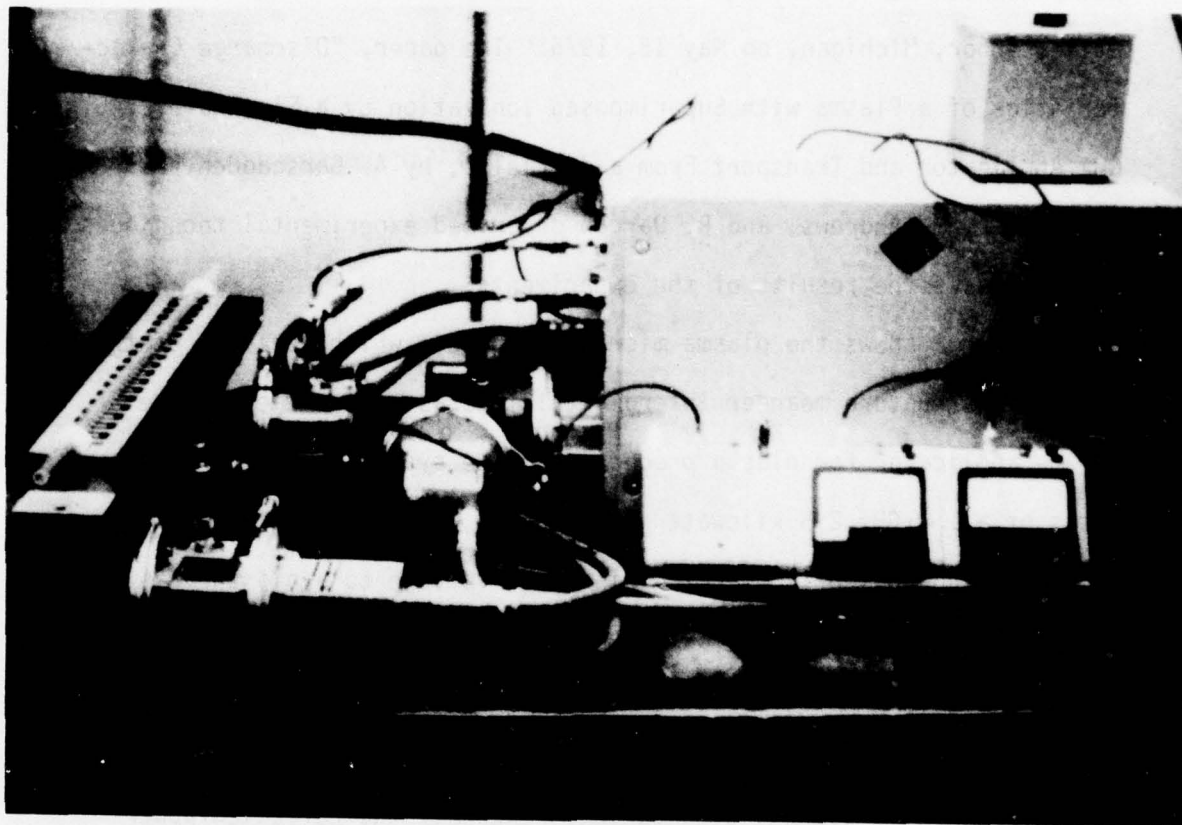


FIGURE 1. GERLING-MOORE 2.45 GHz - 2.5 KWatt MICROWAVE SYSTEM

with a longitudinal flow tube across its active surface.

The applicator's meander title describes exactly the form of the line and it can be simply a milled slot 0.8 cm wide, 3.3 cm deep with a 4.0 cm transverse outside length, having a longitudinal period of 2.5 cm (see Figure 2).^{3,4} The efficiency of the line is sensitive to the dimensions. It will, of course, not propagate dc but can, to first order, be thought of as one-half of a waveguide operating in its fundamental TE_{10} mode, sliced longitudinally and then folded back and forth. The E field then is a maximum at the open edge of the guide and is ideal for applicator purposes. Although the unloaded applicator radiates very little, a protective shield is required with the plasma ignited.

A strapped-bar interdigital slow wave structure has been used by Bosisio et al. as an intermediate pressure plasma source.² Figure 3 shows that the bars are strapped together at the center and only every other bar is connected by the outside rails. Bosisio reports a very uniform production of plasma for longitudinal tubes across the structure.

The unperturbed electric field above the Gerling-Moore applicator has been determined in two ways. Gerling has calculated from the drying rates of thin polymer sheets that the maximum field strength at the surface of the applicator is 5000 volts/cm with 2.5 kwatts incident. Using a dipole antenna probe, the relative electric field versus height above the applicator was determined (see Figure 4). This was done at about thirty positions along the longitudinal axis of the applicator and averaged to obtain this curve. The spread in measurements at various longitudinal positions is indicated by the vertical bar on the

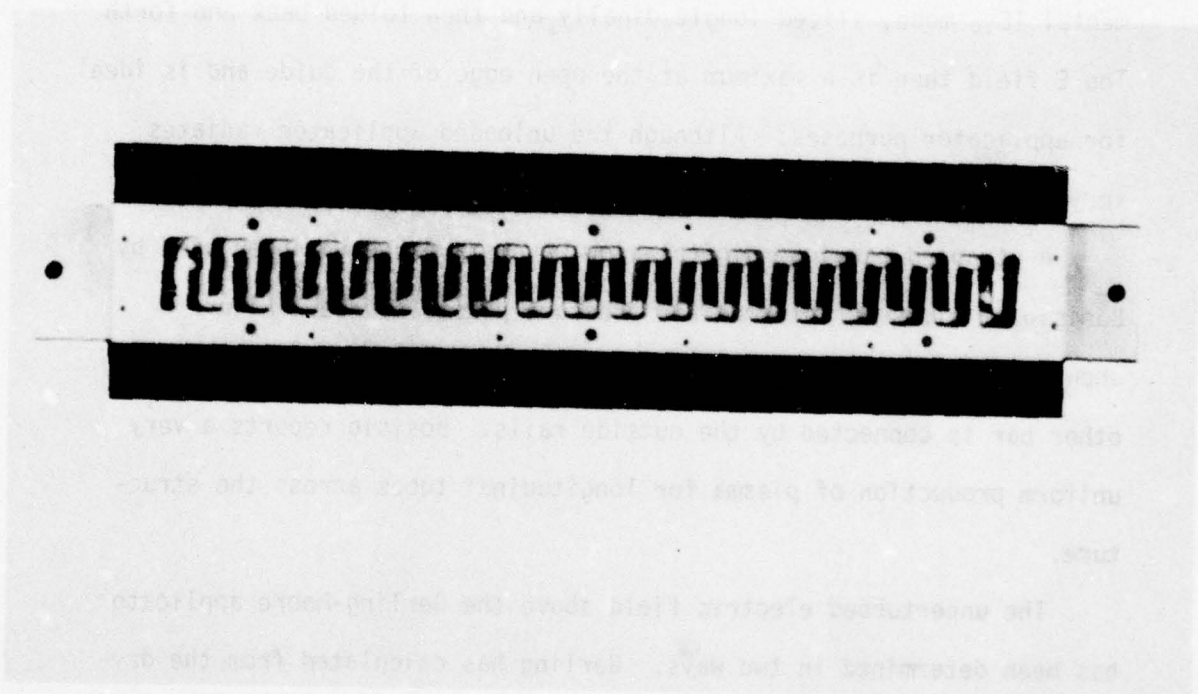


FIGURE 2. INTERDIGITAL SLOW WAVE APPLICATOR

BOSISIO, WEISSFLOCH AND WERTHEIMER: GENERATOR

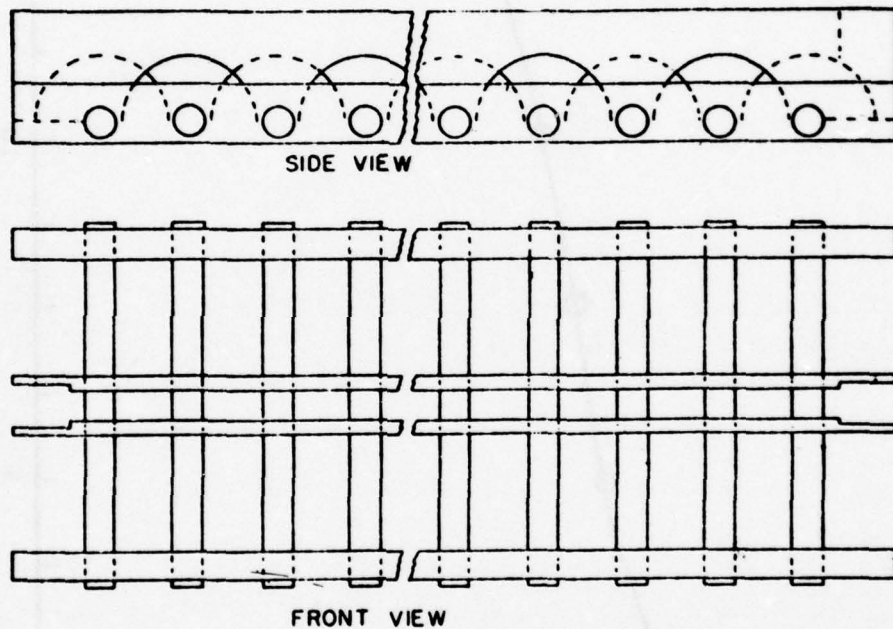


FIGURE 3. STRAPPED-BAR STRUCTURE

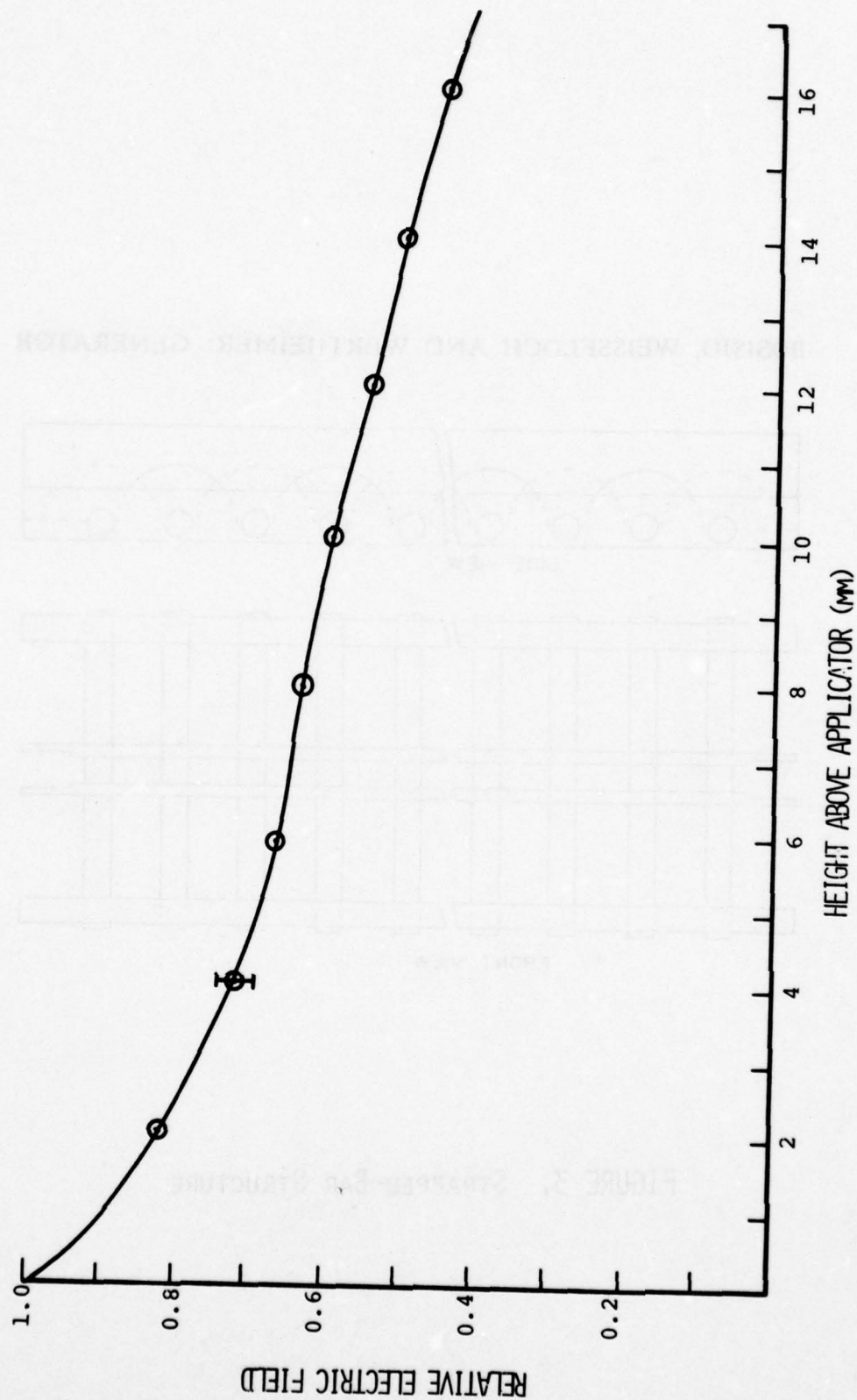


FIGURE 4 - RELATIVE ELECTRIC FIELD VERSUS HEIGHT ABOVE THE APPLICATOR SURFACE

relative field data. Since the E field is proportional to the square root of power, the E field can be determined above the applicator. It should be noted; however, that the diode antenna crystal has finite thickness and the "Zero" height is actually 1 mm above the surface.

A measurement of the E field, independent of the surface drying rate calibration, was obtained by measuring the incident power required for the breakdown in helium at various pressures (see Figure 5). Knowing the distance from the tube axis to the applicator and the falloff of field with height, the breakdown data for helium can be used to estimate the electric field at the closest position of the diode antenna to the applicator surface. This is 3600 volts/cm at 2.5 kwatts or about 30% lower than the drying rate value calibrated at the surface.

In the typical operation of the applicator the plasma absorbs over 60% of the incident power. Thus, one can put 1.5 to 2.0 K watts into flowing helium plasmas in a 1 cm² cross section tube over a broad pressure range of 10 - 200 torr with a few thousand sccm flow rates.

In order to get the most uniform absorption of the microwave power into the plasma, it is necessary to raise the tube up off the applicator surface at the power input end, so that the electric field, which is attenuated as absorption occurs, is nearly constant along the tube. The attenuation due to the height off the surface is just balanced against that due to loss along the tube by properly setting the angle. In Figure 6 exposures were made directly above the applicator surface and show three different tube angles used in breakdown. In the first exposure the tube is on the 45 cm long applicator surface; in the

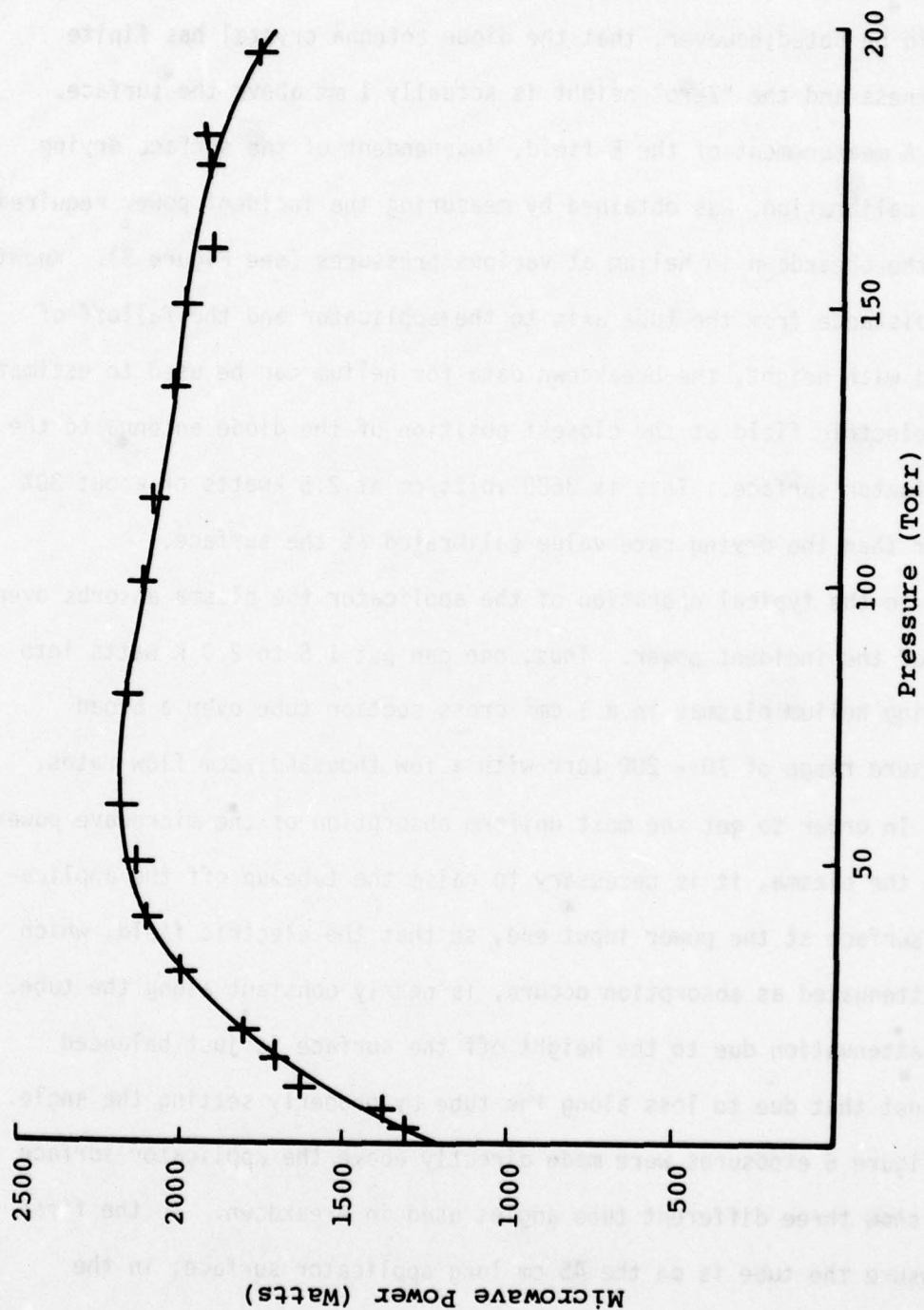


FIGURE 5. APPLICATOR MICROWAVE POWER ABSORBED IN
A HELIUM PLASMA VERSUS PRESSURE



FIGURE 6. HEIGHT ADJUSTMENT OF FLOW TUBE ABOVE APPLICATOR

second exposure the quartz tube at the input power end of the applicator is 3 mm off the surface; in the third exposure the end is at 6 mm off the surface. The optimum height for these conditions was ≈ 8 mm.

The transverse flow configuration mentioned earlier is more uniform than these centered longitudinal exposures indicate. In Figure 7 a comparison of the transverse and longitudinal flow is shown. The exposures were taken directly above the applicator's active surface. When the longitudinal flow tube is shifted parallel over from the center axis of the applicator to run along the end of the interdigital spacing on one side, Figure 7A shows that the low field locations in the center interchange and are high field positions on the edge. Figures 7B and 7C show the transverse flow shifted one-half interdigital spacing with respect to each other. Therefore, Figure 7 shows that in the two different transverse positions relative to the interdigital spacings, there is still breakdown across the entire tube diameter.

2. ELECTRON DENSITY MEASUREMENTS

Several experimental arrangements of the slow wave structure meander interdigital line as a large volume applicator for plasma production in argon and helium were tried. Measurements of the electron density in helium were made. Measurements of the electron density in argon; however, were found to be much more difficult to obtain with reasonable reproducibility. The problems encountered in attempting the argon measurements will be discussed later in this report.

The flow tube used for measurements is shown in Figure 8. The electrode assembly consisted of two OFHC copper rods machined to slide into the 4 mm i.d. quartz sidearms and press fit into a Swagelok end

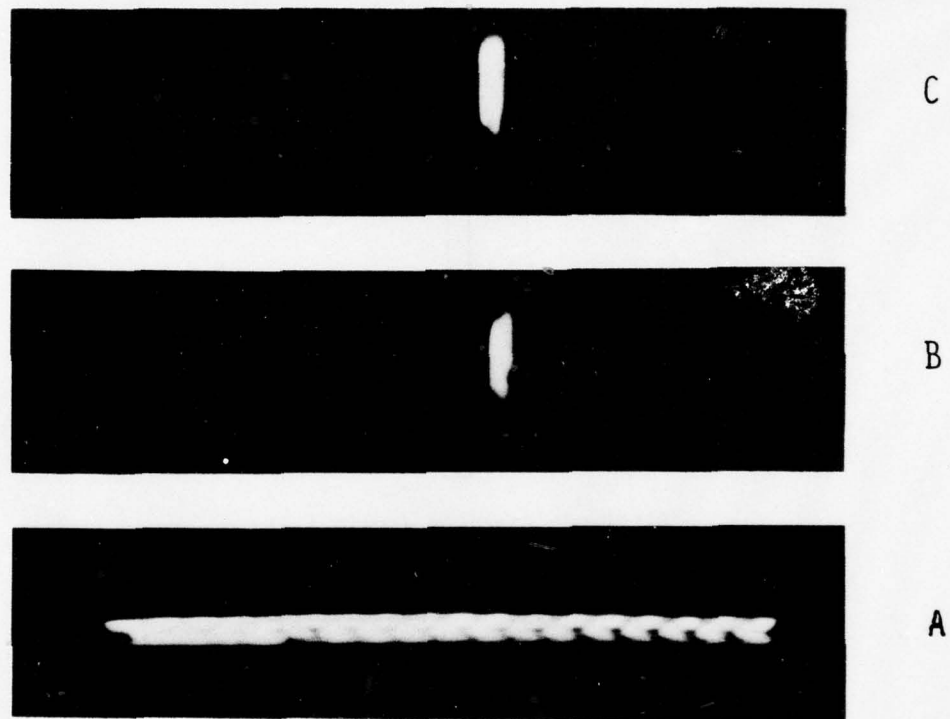


FIGURE 7. TRANSVERSE FLOW POSITIONS

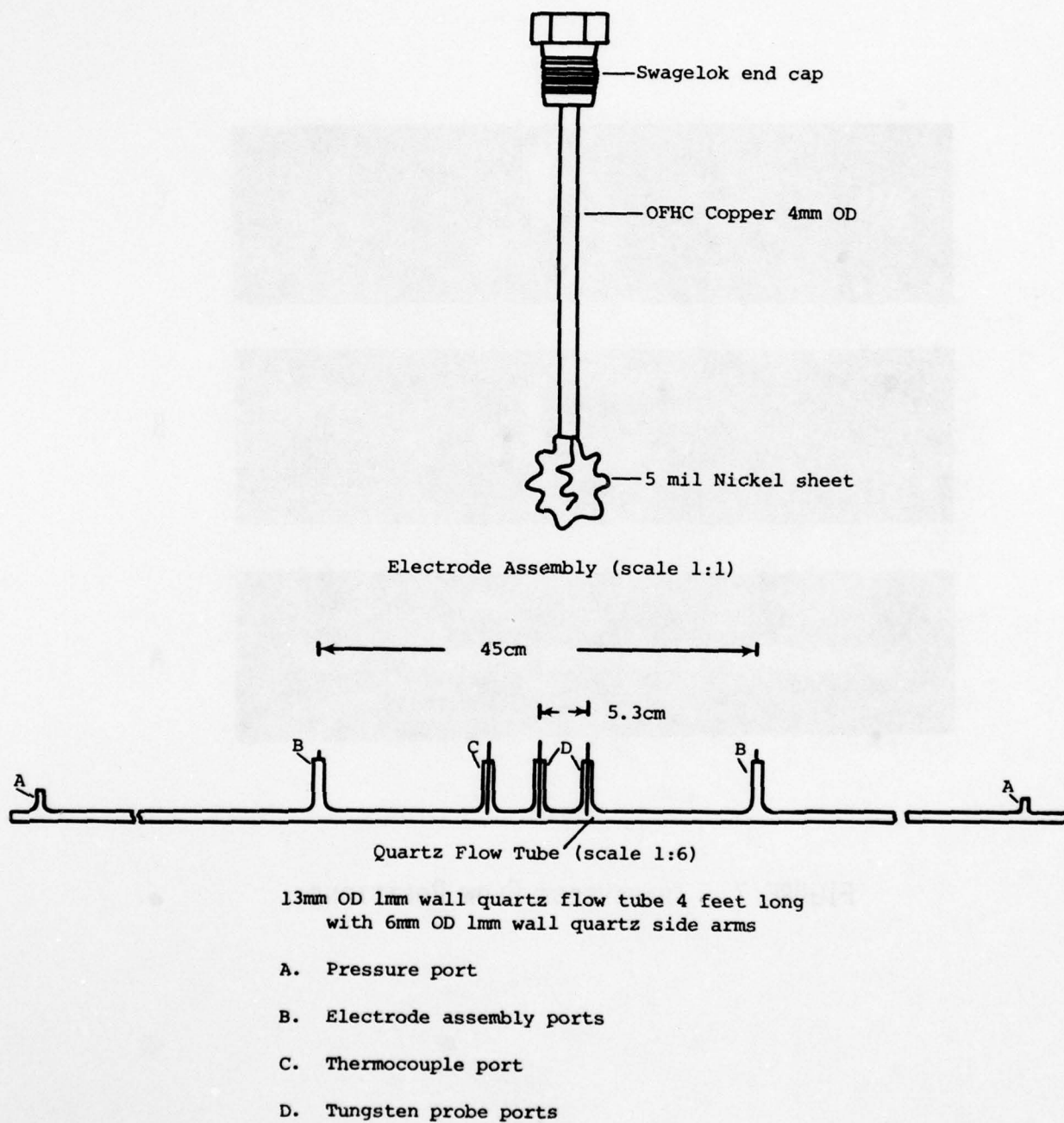


FIGURE 8 - FLOW TUBE AND ELECTRODE ASSEMBLY

cap with teflon ferrules used to seal to the sidearm tube. A 5 mm wide strip of 5 mil thick nickel sheet was fabricated into a "honeycomb" type of electrode by corrugating the sheet between the teeth of two gears and spiraling the metal. A hole was punched in the nickel and the copper rod of the electrode was press fit into the nickel electrode. Two 5 mil tungsten probes, separated by approximately the distance of two interdigital spacings, i.e., 2 inches, were used to make measurements of the applied dc field in the plasma. The probes were sealed to the tube with Torr Seal epoxy. The tube was placed along the applicator so that there was no transverse movement of the tube with respect to the applicator, but the tube could be raised or lowered at the microwave input (upstream) end of the applicator.

Several experimental arrangements were used to obtain data on electron densities. Two of these arrangements will be discussed here.

Figure 9 shows the first arrangement used to obtain data. A voltage ramp with an amplitude of ± 50 V and a period of 60 seconds was applied to the electrodes. The current created by the external field in the microwave-produced plasma was monitored from a $10\ \Omega$ resistor. A Preston Differential amplifier with a high input impedance, greater than $100\ \text{M}\Omega$ and a common mode rejection greater than 10^4 was used to monitor the dc field in the plasma.

To eliminate a dc offset problem, the microwaves were pulsed. Figure 10 shows the experimental arrangement used. The microwave power applied to the plasma was pulsed using a Sanders 200 watt microwave switch with a rise time less than a microsecond,⁵ and a repetition

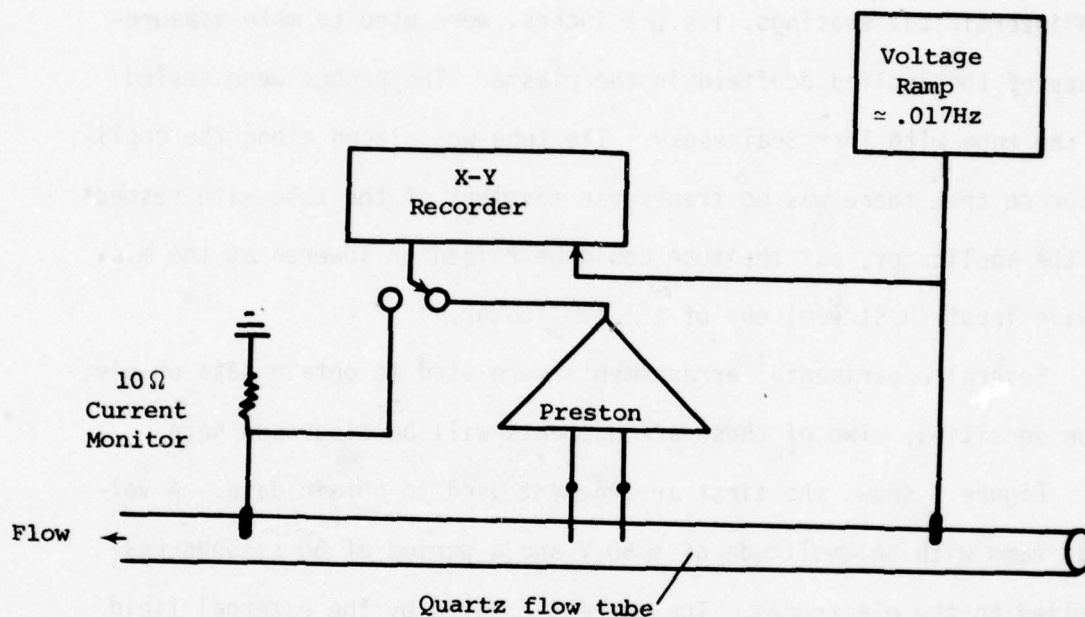


FIGURE 9 - INSTRUMENTATION FOR I-V CHARACTERISTICS OF HE AND AR

rate greater than 50 Hz. The voltage ramp applied to the plasma was the same as in Figure 9. A PAR boxcar integrator was used to set the aperture time for the measurement of the plasma electric drift field taken from the high impedance probes.

In this arrangement the microwaves were on for most of the 50 Hz period and turned off for a short time. This was necessary in order to get repetitive re-ignition of the plasma at low powers. It was discovered that this off-time, at the lowest powers of 15 watts and 5 torr of argon, could be extended to at least 300 microseconds. However, this method for probe measurements did not prove profitable because there was no adequate differential amplifier readily available. The amplifier would have to have a frequency response on the order of 10 MHz, a high input impedance of about 100 M Ω , a common mode rejection greater than 10^3 , and a voltage input capability of ± 10 volts.

Measurements of the electron density in helium using the arrangement shown in Figure 9 provided a correction to earlier measurements⁴ by eliminating electrode sheath potential drop and using pure drift plasma electric fields. For argon, however, the measurement proved much more difficult.

With no dc voltage applied to the plasma, there was a voltage offset between the probes that was found to be dependent on pressure, flow, microwave power, and position of the flow tube with respect to the applicator. The voltage offset between the probes with no voltage applied to the electrodes changed strongly with small changes of the tube height off the applicator, and the longitudinal position of the

tube with respect to the applicator. The offset voltage changed only slightly with small changes of the transverse position of the tube with respect to the applicator.

This voltage offset varied from approximately -10 V to +10 V and could be varied by changing the position of the tube with respect to the applicator. The electric field corresponding to a 10 volt offset between the probes is about 2 V/cm. Because of the difference in conductivity for helium and argon, typical measurements of the electric field between the probes for helium was 0.1 V/cm and for argon was 5×10^{-3} V/cm. Thus, for most measurements made on argon, the field between the probes with no voltage applied to the electrodes is much greater than the field produced from the applied voltage.

To investigate the possibility that the measured offset was not an effect of the microwave leakage on the electronic measuring devices, a Hewlett-Packard 431C microwave power meter was used to monitor the amount of the microwave power transmitted along the coaxial cables used to connect the equipment. The transmitted microwave power level in the coaxial cables was about one microwatt at 100 watts input to the applicator with or without a plasma produced in the flow tube. The offset voltage between the probes was only present when a plasma was produced in the flow tube. However, the microwave power transmitted through the cables to the instruments was the same with or without a plasma present. Therefore, it was concluded that the measured offset voltage was produced between the probes, and was not a reading produced from the microwaves interfering with the electronic measuring devices.

When attempting to obtain measurements of the electron density in argon, using the arrangement of Figure 9, it was found that the probe measurements could be made only if the tube was aligned on the applicator so that there was approximately zero voltage between the probes with no voltage applied to the electrodes. However, this did not represent a satisfactory solution to the problem since the uniformity of the plasma produced by microwave breakdown in the applicator is dependent on the height of the tube off the applicator at the power input end of the applicator.² Even though it was possible to eliminate the voltage offset between the probes, there was still the problem of having a nonuniform plasma produced, such that the plasma density was much higher at one electrode than the other. This was coupled with the problem of mounting the tube so that it could be adjusted with respect to the applicator, but would still be extremely stable during measurements to eliminate changes of one part in ten thousand in the offset voltage while measurements of the current and probe voltage were being taken.

In attempting to eliminate these problems several arrangements were used, culminating in the set-up shown in Figure 10. If the voltage offset between the probes was due to a rectification of the microwave power by the plasma sheaths, then pulsing the microwaves and making the field measurements when the microwave power was off would eliminate the voltage offset.

On the other hand, diffusion fields from plasma inhomogeneities would not immediately dissipate when the microwaves were turned off. Although the differential amplifier response time was not fast enough to

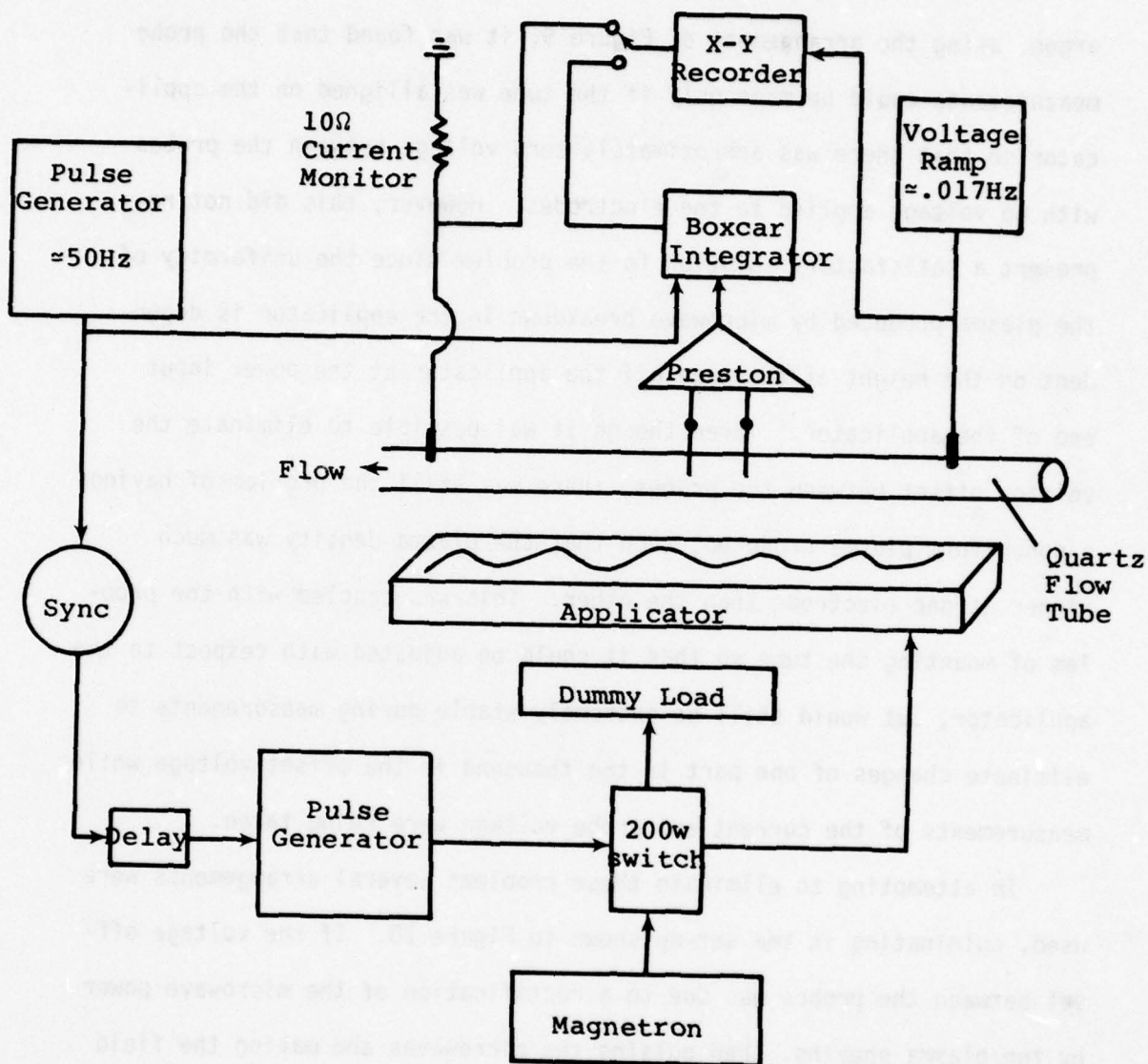


FIGURE 10. INSTRUMENTATION FOR I-V CHARACTERISTICS OF He AND Ar IN A PULSED DISCHARGE

follow the pulse of the microwave power, the large magnitude of the offset favored the local diffusion field explanation.

In a microwave produced plasma with an external applied field for transport, there is a current density produced given by

$$j = N_e e V_d \quad (1)$$

where

j is current density

N_e is electron density

e is electron charge

V_d is electron drift velocity

and

$$V_d = \mu_e E \quad (2)$$

where

μ_e is the electron mobility

and

E is the applied field.

Since the plasma is produced totally by the effective microwave field, \tilde{E}_{eff} , and is not a function of the small electric field, E_{DC} , which is applied just for transport of electrons and ions to obtain current measurements, then the mobility of the electrons $\mu_e[\tilde{E}_{eff}]$ is a function of the applied microwave field only, and the drift velocity in Eq. (2) is the product of the mobility and electric field, E_{DC} , or

$$V_d = (\mu_e [\tilde{E}_{eff}]) E_{DC} . \quad (3)$$

Then Eq. (1) can be written as

$$j = N_e e (\mu_e [\tilde{E}_{eff}]) E_{DC} . \quad (4)$$

Since the microwave power density absorbed in the plasma is given by⁶

$$W = N_e e \mu_e \tilde{E}_{eff}^2 \quad (5)$$

then

$$\tilde{E}_{eff} = \sqrt{\frac{W}{N_e e \mu_e}} . \quad (6)$$

Substitution of Eq. (4) in Eq. (6) gives

$$\tilde{E}_{eff} = \sqrt{\frac{E_{DC} W}{j}} . \quad (7)$$

The effective microwave field (\tilde{E}_{eff}) calculated from Eq. (7) can then be used with the data given by Huxley and Crompton⁷ for helium and by Gilardini⁶ for argon to determine the mobility of the electrons. The electric field (E_{DC}) is determined from the probe measurements and the current density is determined from the measurements of the current through the 10 Ω resistor. The electron density can then be determined by rearranging Eq. (4) to

$$N_e = \frac{j}{e (\mu_e [\tilde{E}_{eff}]) E_{DC}} . \quad (8)$$

Figure 11 shows data taken for helium using the configurations of Figure 9. Curve 1 is the current-voltage measured between the electrodes. Curve 2 is the electrode voltage plotted against the probe voltage. From these curves for helium:

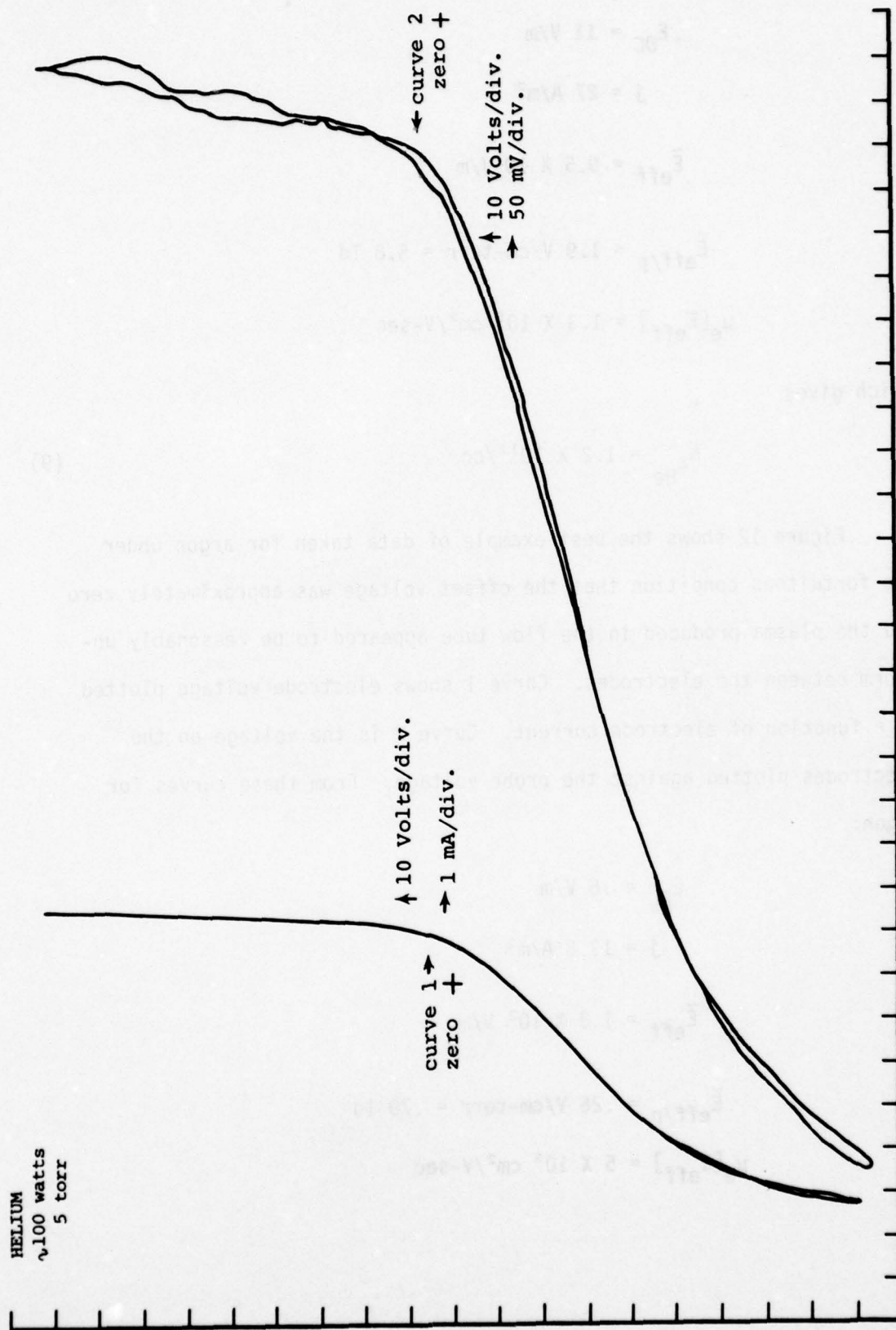


FIGURE 11 - HELIUM I-V CHARACTERISTIC CURVE

$$E_{DC} = 11 \text{ V/m}$$

$$j = 27 \text{ A/m}^2$$

$$\tilde{E}_{eff} = 9.5 \times 10^2 \text{ V/m}$$

$$\tilde{E}_{eff/p} = 1.9 \text{ V/cm-torr} = 5.8 \text{ Td}$$

$$\mu_e[E_{eff}] = 1.3 \times 10^5 \text{ cm}^2/\text{V-sec}$$

which gives

$$N_{e_{He}} = 1.2 \times 10^{12}/\text{cc} \quad (9)$$

Figure 12 shows the best example of data taken for argon under the fortuitous condition that the offset voltage was approximately zero and the plasma produced in the flow tube appeared to be reasonably uniform between the electrodes. Curve 1 shows electrode voltage plotted as a function of electrode current. Curve 2 is the voltage on the electrodes plotted against the probe voltage. From these curves for argon:

$$E_{DC} = .6 \text{ V/m}$$

$$j = 12.5 \text{ A/m}^2$$

$$\tilde{E}_{eff} = 1.3 \times 10^2 \text{ V/m}$$

$$\tilde{E}_{eff/p} = .26 \text{ V/cm-torr} = .79 \text{ Td}$$

$$\mu_e[E_{eff}] = 5 \times 10^5 \text{ cm}^2/\text{V-sec}$$

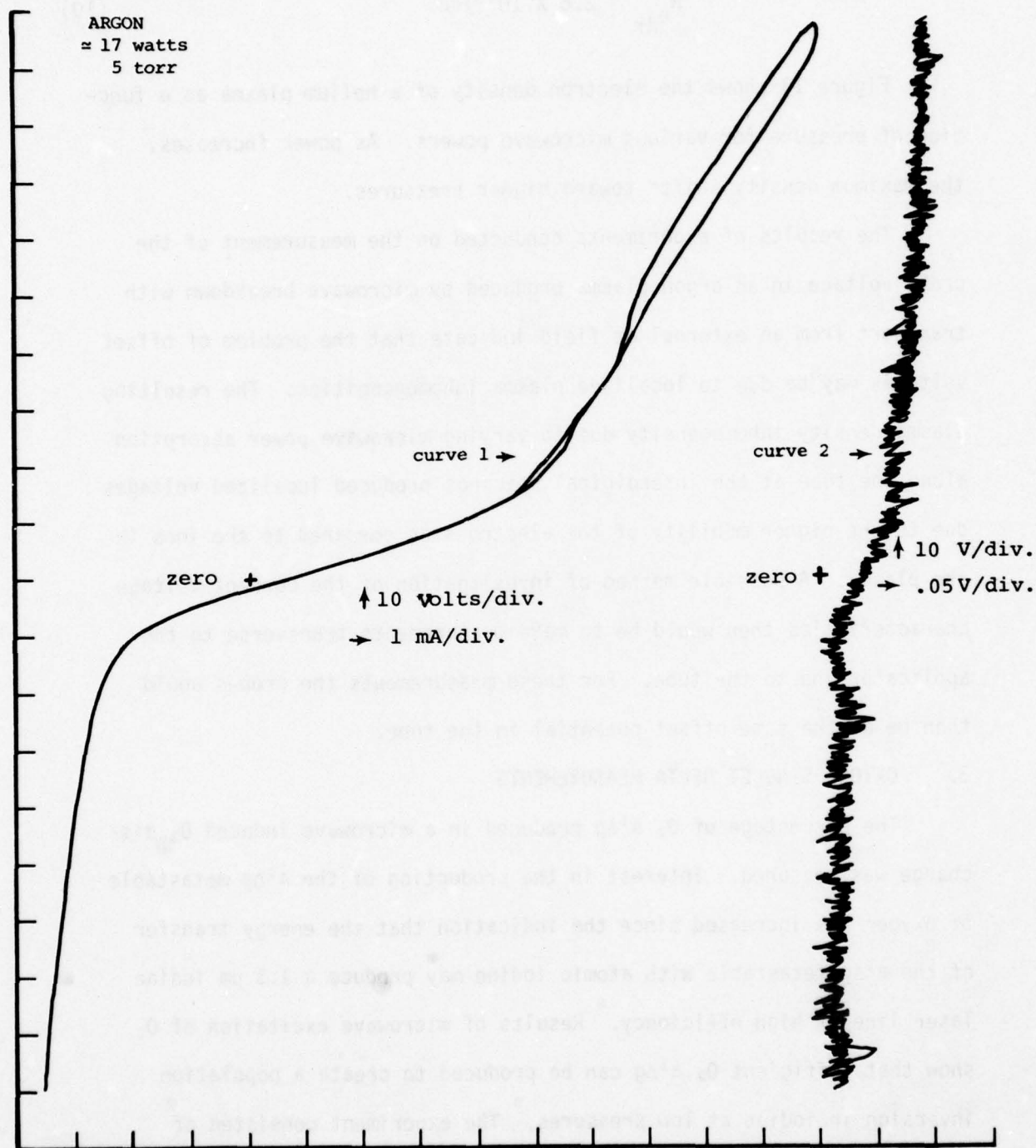


FIGURE 12 - ARGON I-V CHARACTERISTIC CURVE

which gives

$$N_{eAr} = 2.6 \times 10^{12}/cc \quad (10)$$

Figure 13 shows the electron density of a helium plasma as a function of pressure for various microwave powers. As power increases, the maximum density shifts toward higher pressures.

The results of experiments conducted on the measurement of the probe voltage in an argon plasma produced by microwave breakdown with transport from an external dc field indicate that the problem of offset voltages may be due to localized plasma inhomogeneities. The resulting plasma density inhomogeneity due to varying microwave power absorption along the tube at the interdigital spacings produced localized voltages due to the higher mobility of the electrons as compared to the ions in the plasma. A possible method of investigation of the current-voltage characteristics then would be to make measurements transverse to the applicator and to the tube. For these measurements the probes would then be at the same offset potential in the tube.

3. OXYGEN SINGLET DELTA MEASUREMENTS

The percentage of O_2 $a^1\Delta_g$ produced in a microwave induced O_2 discharge was measured. Interest in the production of the $a^1\Delta_g$ metastable of oxygen has increased since the indication that the energy transfer of the $a^1\Delta_g$ metastable with atomic iodine may produce a 1.3 μm iodine laser line of high efficiency.⁸ Results of microwave excitation of O_2 show that sufficient O_2 $a^1\Delta_g$ can be produced to create a population inversion in iodine at low pressures.⁹ The experiment consisted of the use of both a McCarroll-type Evenson cavity and the Gerling-Moore

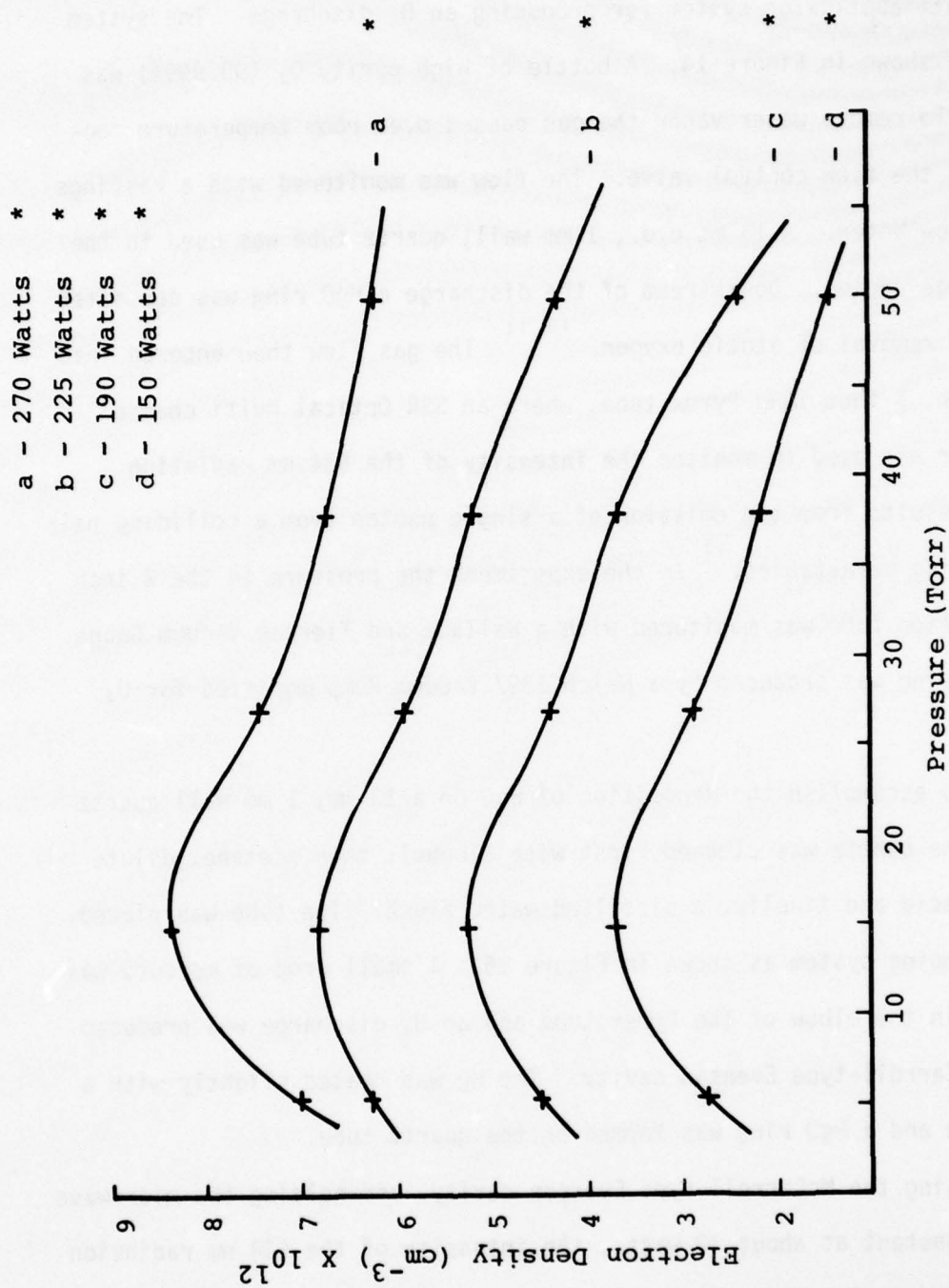
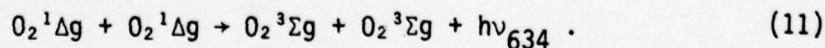


FIGURE 13. ELECTRON DENSITY IN HELIUM AS A FUNCTION OF PRESSURE FOR SEVERAL MICROWAVE POWERS

2.5 kwatt applicator system for producing an O_2 discharge. The system used is shown in Figure 14. A bottle of high purity O_2 (99.999%) was used. To remove water vapor the gas passed over room temperature zeolite to the flow control valve. The flow was monitored with a Hastings Mass Flow Meter. A 13 mm o.d., 1 mm wall, quartz tube was used in the discharge region. Downstream of the discharge a HgO ring was deposited for the removal of atomic oxygen.^{10,11} The gas flow then entered into a 2 inch, 5 foot long Pyrex tube, where an SSR Optical Multi-channel Analyzer was used to monitor the intensity of the 634 nm radiation which results from the emission of a single photon from a colliding pair of O_2 $a^1\Delta_g$ metastables.¹² In the experiment the pressure in the 2 inch observation tube was monitored with a Wallace and Tiernan Vacuum Gauge. The pumping was produced by a Welch 1397 Vacuum Pump modified for O_2 use.

To accomplish the deposition of HgO on a 13 mm, 1 mm wall quartz tube, the quartz was cleaned first with alcohol, then acetone, dilute nitric acid and finally, a distilled water flush. The tube was placed in a pumping system as shown in Figure 15. A small drop of mercury was placed in the elbow of the Pyrex tube and an O_2 discharge was produced by a McCarroll-type Evenson cavity. The Hg was heated slightly with a heat gun and a HgO ring was formed on the quartz tube.

Using the McCarroll-type Evenson cavity, and holding the microwave power constant at about 70 watts, the intensity of the 634 nm radiation from the emission of a colliding pair of O_2 $a^1\Delta_g$ was measured, i.e.,



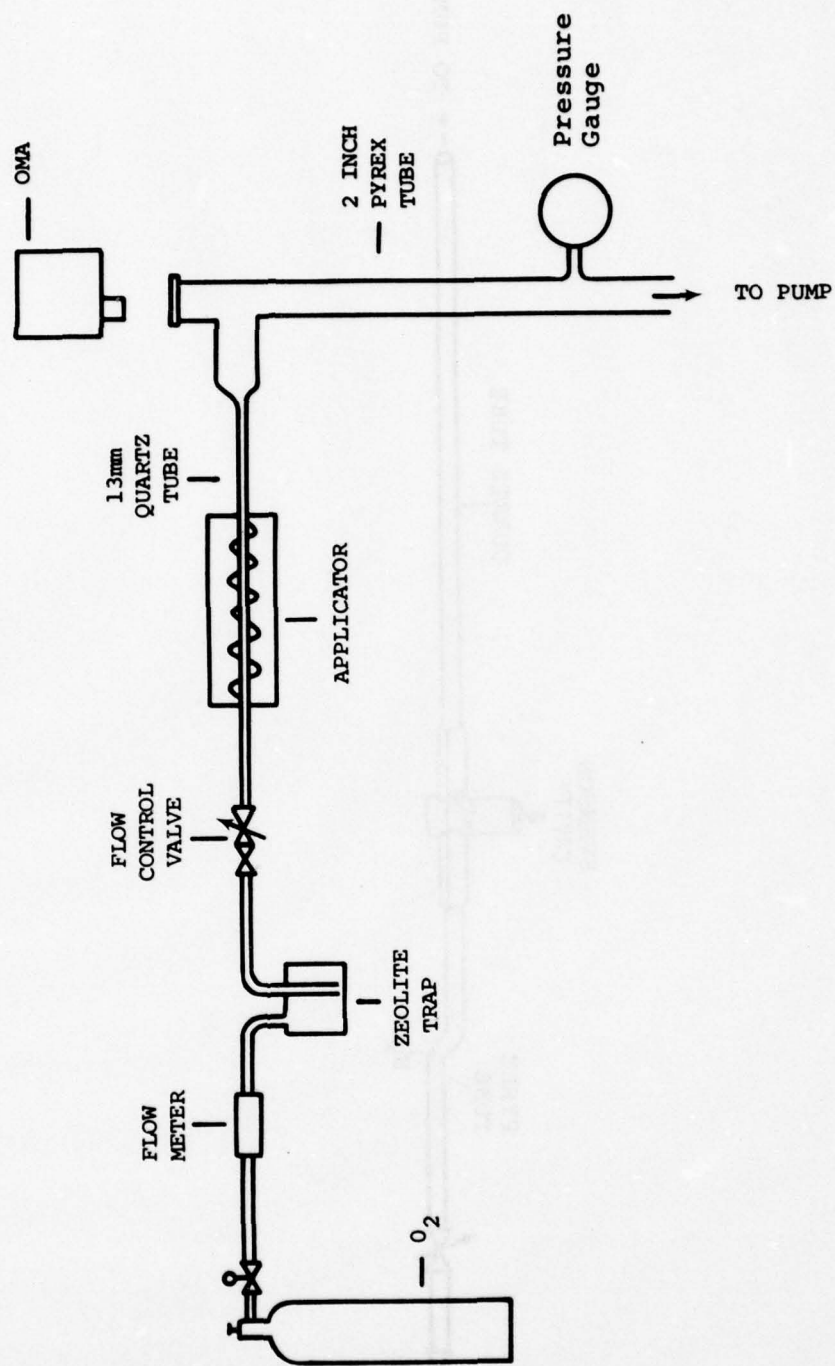


FIGURE 14 - MICROWAVE DISCHARGE SYSTEM FOR THE PRODUCTION OF $O_2^{1\Delta}$

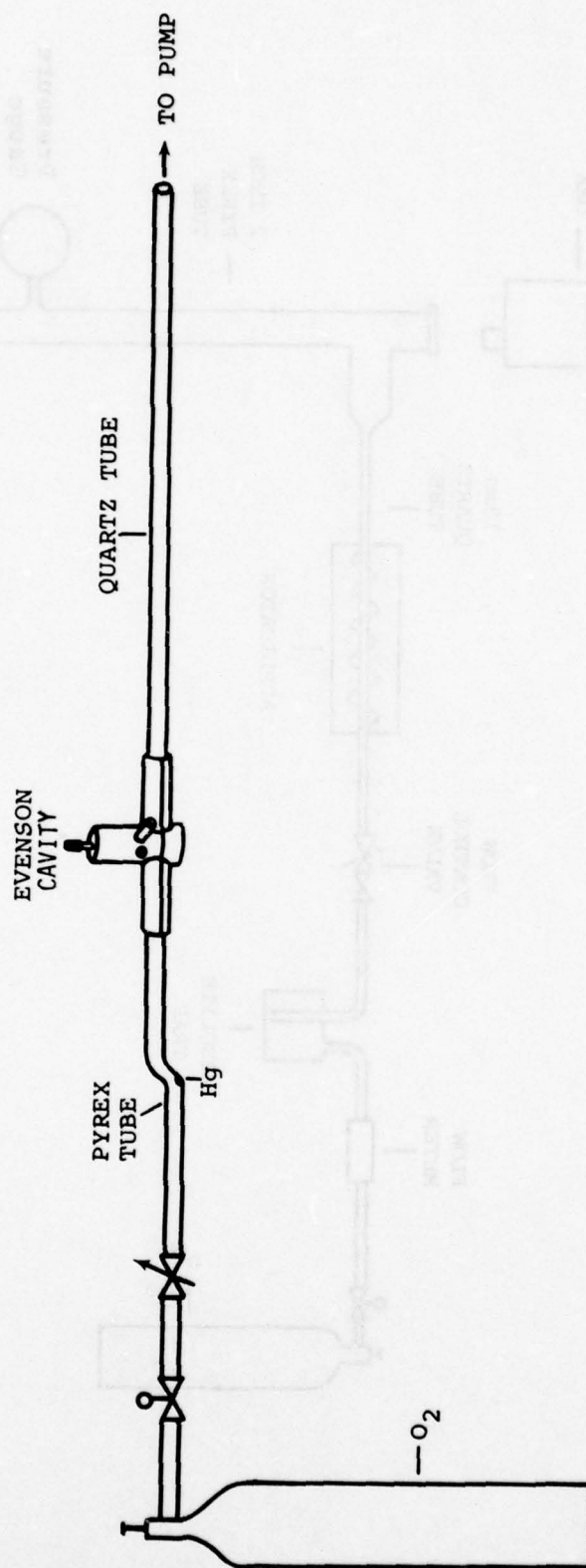


FIGURE 15. SYSTEM USED FOR DEPOSITION OF HgO ON A QUARTZ TUBE

The proportionality of the emission to the square of the concentration of the $O_2^1\Delta g$ metastable has been shown by several means.¹¹ The percent of the molecules in the $^1\Delta g$ state is proportional to the square root of the measured intensity and inversely proportional to the pressure, or

$$\%O_2 \text{ in } ^1\Delta g \text{ state} \propto \frac{\sqrt{I_{634}}}{P} . \quad (12)$$

The relative number of $O_2^1\Delta g$ produced by a 70 watt microwave discharge as a function of pressure is shown in Figure 16. This curve correlates very well with the 70 watt data report by A. MacKnight and P. Modreski,⁹ which serves as an absolute calibration of the percent of $O_2^1\Delta g$ produced. This corresponds to a production of about 25% at low pressures.

The interdigital applicator system used in place of the McCarroll-type cavity, Figure 14, resulted in 634 nm radiative intensities on the same order as observed with the Evenson cavity (see Figure 16). The applicator was also used to obtain data on the 634 nm intensity as a function of applied microwave power. The average of 5 measurements were plotted. The results, Figure 17, show a peak in the intensity of the $O_2^1\Delta g$ at about 100 to 120 watts of the microwave power.

These results obtained with the slow wave interdigital applicator were with a longitudinal flow. This type of configuration may give rise to a temperature increase of the gas at higher microwave power, such that optimum power loading is not achieved, since the gas is flowing along the applicator for the entire length of the discharge. In

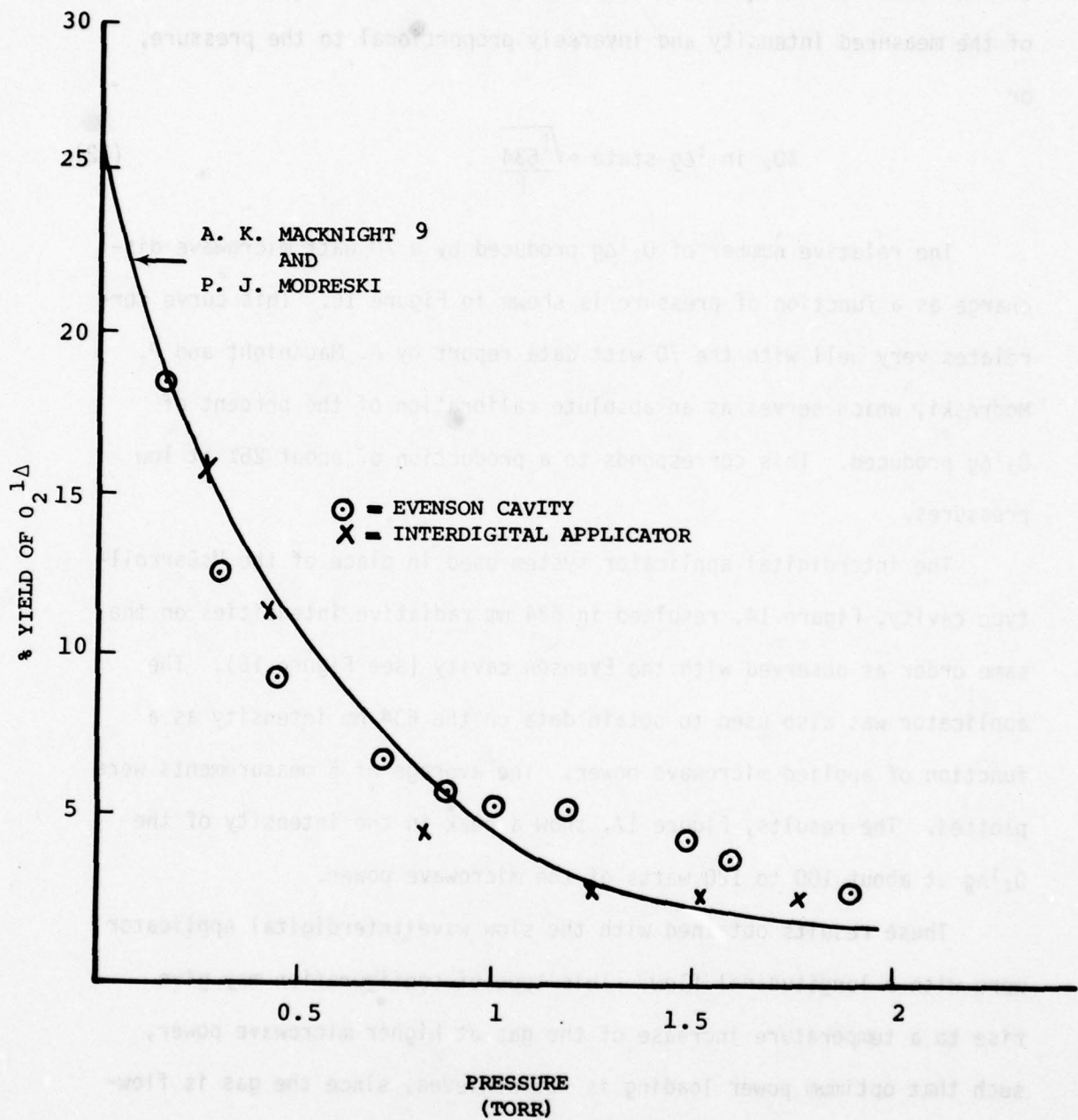


FIGURE 16. % YIELD OF $O_2^1\Delta_g$ IN A 70 WATT MICROWAVE DISCHARGE AS A FUNCTION OF PRESSURE

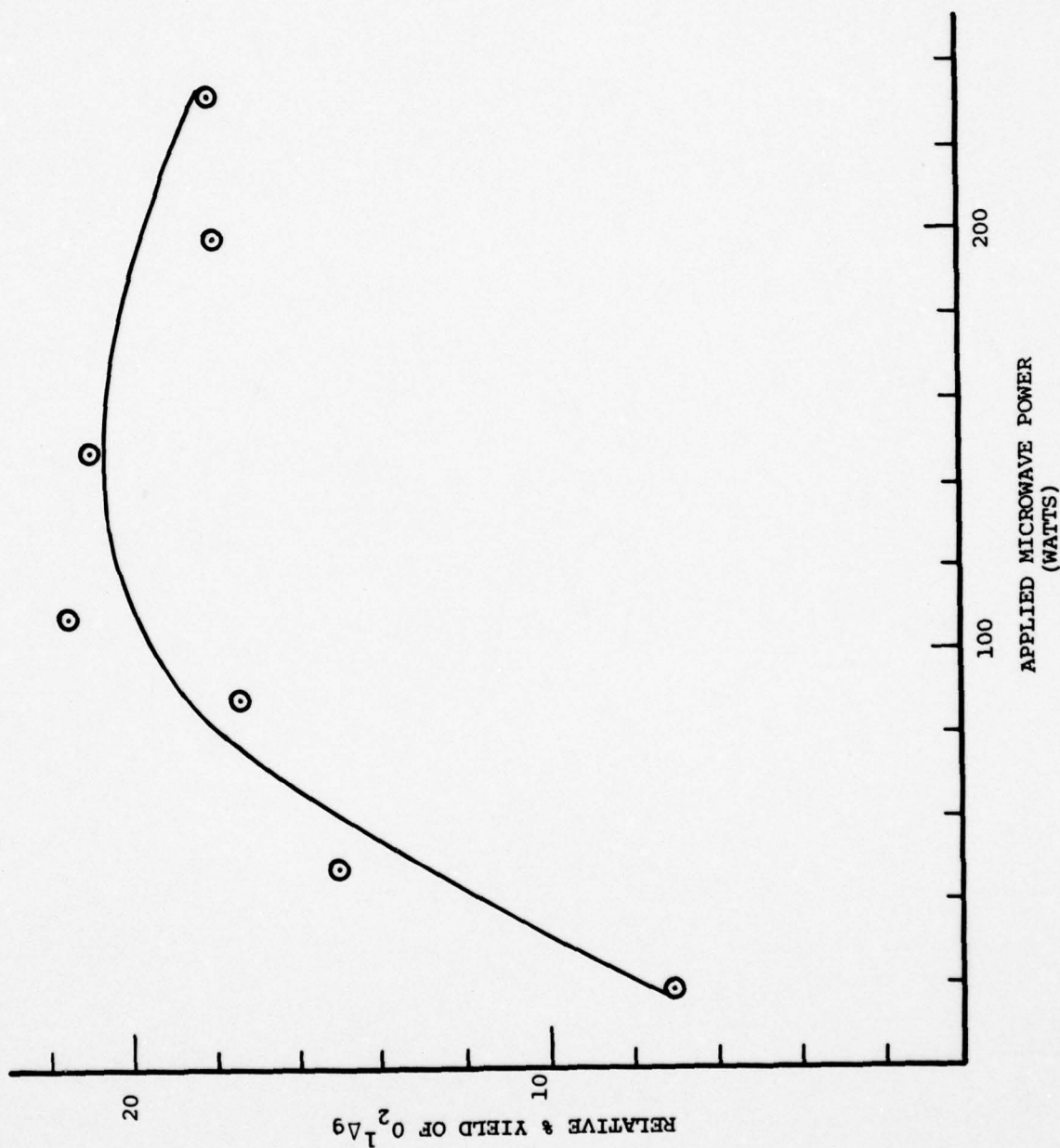
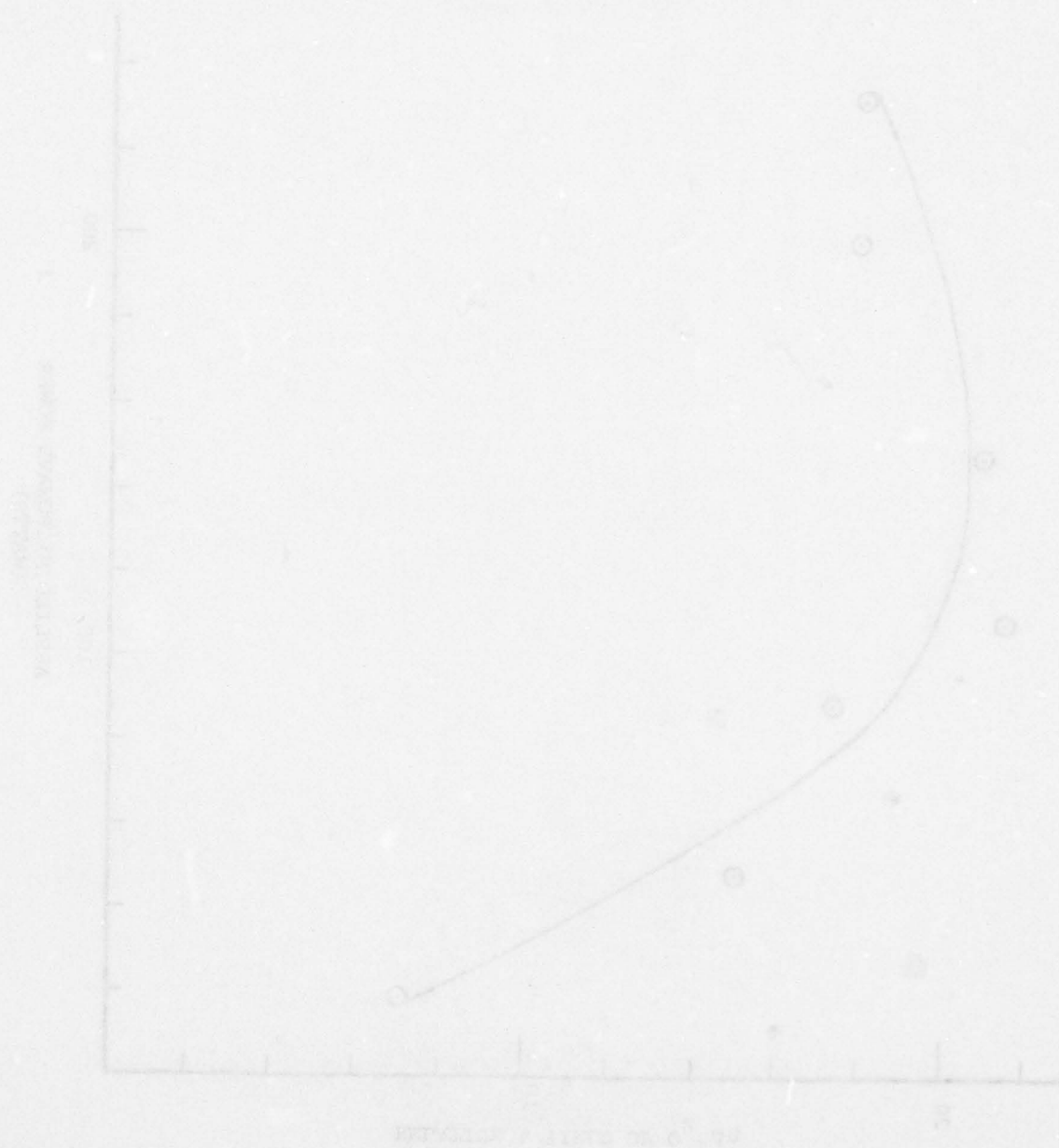


FIGURE 17 - RELATIVE % YIELD OF $O_2^1\Delta_g$ AS A FUNCTION OF MICROWAVE POWER

a transverse flow configuration where the applicator is perpendicular to the gas flow, the gas would be in the discharge region for a much shorter length of time, and an increase in the percent of $O_2^1\Delta g$ production may be achieved at the same power levels.

FIGURE 10 - RELATIVE $O_2^1\Delta g$ YIELD AS A FUNCTION OF DISCHARGE POWER



SECTION III

SANDWICH APPLICATOR SYSTEM

1. SYSTEM DESCRIPTION

In order to obtain higher microwave power (5 kW) input into the plasma medium and a more uniform microwave field, a "sandwich" of two applicators was designed. A picture of the "sandwich" applicator is shown in Figure 18. The basic concept is that two Gerling-Moore slow wave structure interdigital applicators are used in an aluminum shielding box, with the active surfaces parallel and facing each other. Threaded rods separate the applicators, support the upper applicator, and allow the perpendicular distance between the active surfaces to be varied by the vertical movement of the upper applicator, permitting the upper active surface longitudinal movement of more than one interdigital spacing with respect to the lower fixed applicator.

Shielding of microwave radiation from around the movable upper applicator was accomplished by a plate attached to the applicator with finger contact along the sides of the shielding box. The sides of the box have a 20 inch long by 2 inch high slot covered with perforated 20 gauge aluminum sheet for observation of the discharge. The ends of the box have one inch slots for insertion of longitudinal flow tubes. Copper screen around the longitudinal flow tube was attached to the ends of the box to act as a wave guide below cutoff.

2. OXYGEN ATOM PRODUCTION

Molecules of oxygen have been disassociated into atomic species for use in several laser systems.¹³ This experimental system was used

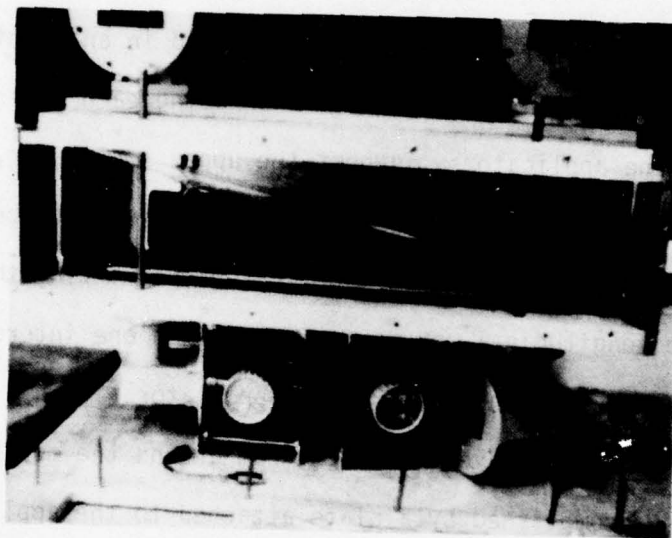


FIGURE 18. "SANDWICH" APPLICATOR

to investigate the possibility of employing the slow wave structure, interdigital meander line as a microwave applicator for the production of atomic oxygen for laser systems. With the "sandwich" applicator system discussed above, measurement of the oxygen atom production from a uniform high power microwave field incident on an oxygen flow was performed.

The microwave applicator system used for atom production experiments is shown in Figure 19. Two Gerling-Moore magnetron power supplies with controllers were used to supply 2.5 kW each of low ripple microwave power. A check of the frequency of the two magnetrons gave the following results. Supply 177 had a frequency of $2.441 \pm .001$ GHz, and supply 212 had a frequency of $2.448 \pm .002$ GHz.

The wave form of the microwave power output of the Gerling-Moore power supplies was examined. The output of the crystal detector of the microwave power meter was measured on a Tektronix 1A7A differential amplifier. For power levels up to 500 watts, the magnetrons cut off and on. At full power, 2.5 kwatts, the ripple was reduced to about 15% peak to peak from both magnetrons with the buck-boost on the power line of supply 177.

A comparison check of the calibration of the microwave power meters was performed. All meters read within 5% of calibration.

Two Airtron three-port circulators were modified to run water cooled with 2.5 kW of 2.45 GHz microwave power transmitted and reflected with no overheating or reflection back to the magnetrons. The dummy loads were tuned so that less than 10 watts were reflected from the water cooled loads with 1000 watts applied with quartz tubing replacing

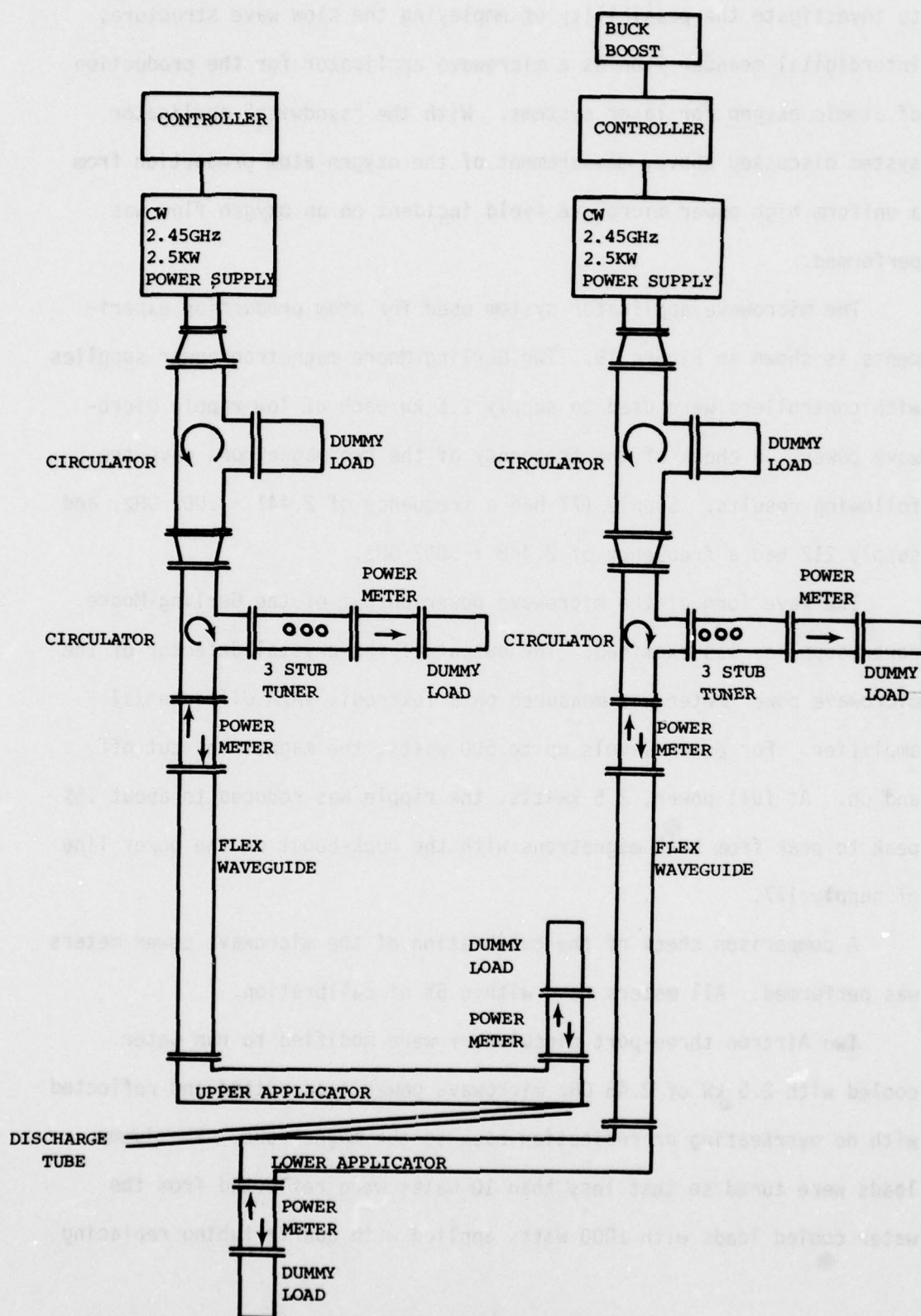


FIGURE 19 - SANDWICH APPLICATOR SYSTEM

the polystyrene previously used in the loads.

Three-port circulators with loads were used as isolators to protect the magnetrons from reflected power and to allow the system to be operated at full power output to minimize the ripple of the microwave system. The power output of each such isolated supply went through a three-port circulator to a three-stub tuner. The power reflected from the tuners was directed by W284 waveguide to the input of the slow wave structure interdigital applicators. This allows the power applied to the plasma to be controlled as determined by the reflection off of the three-stub tuner while the power supplies are operating at maximum output and thus minimum ripple.

Figure 20 shows the flow system used for oxygen atom production. The molecular oxygen and helium flows are measured by Hastings mass flow meters. The system pressure is measured with a Wallace and Tiernan gauge. The oxygen flows over a reservoir of distilled water which adds 0.6% water vapor to the one atmosphere oxygen. A titration tube is used to inject NO_2 into the flow to determine the percent of oxygen atom production from the plasma produced by the microwave field in the sandwich applicator.

The reaction of atomic oxygen with NO_2 produces a green fluorescence. When this fluorescence disappears, the oxygen atom flow is equal to the NO_2 flow. The reactions below proceed such that when there is a greater number of oxygen atoms than NO_2 molecules, the green fluorescence is produced by the second reaction, but when there are an equal or greater number of NO_2 molecules, the oxygen atoms are depleted by the

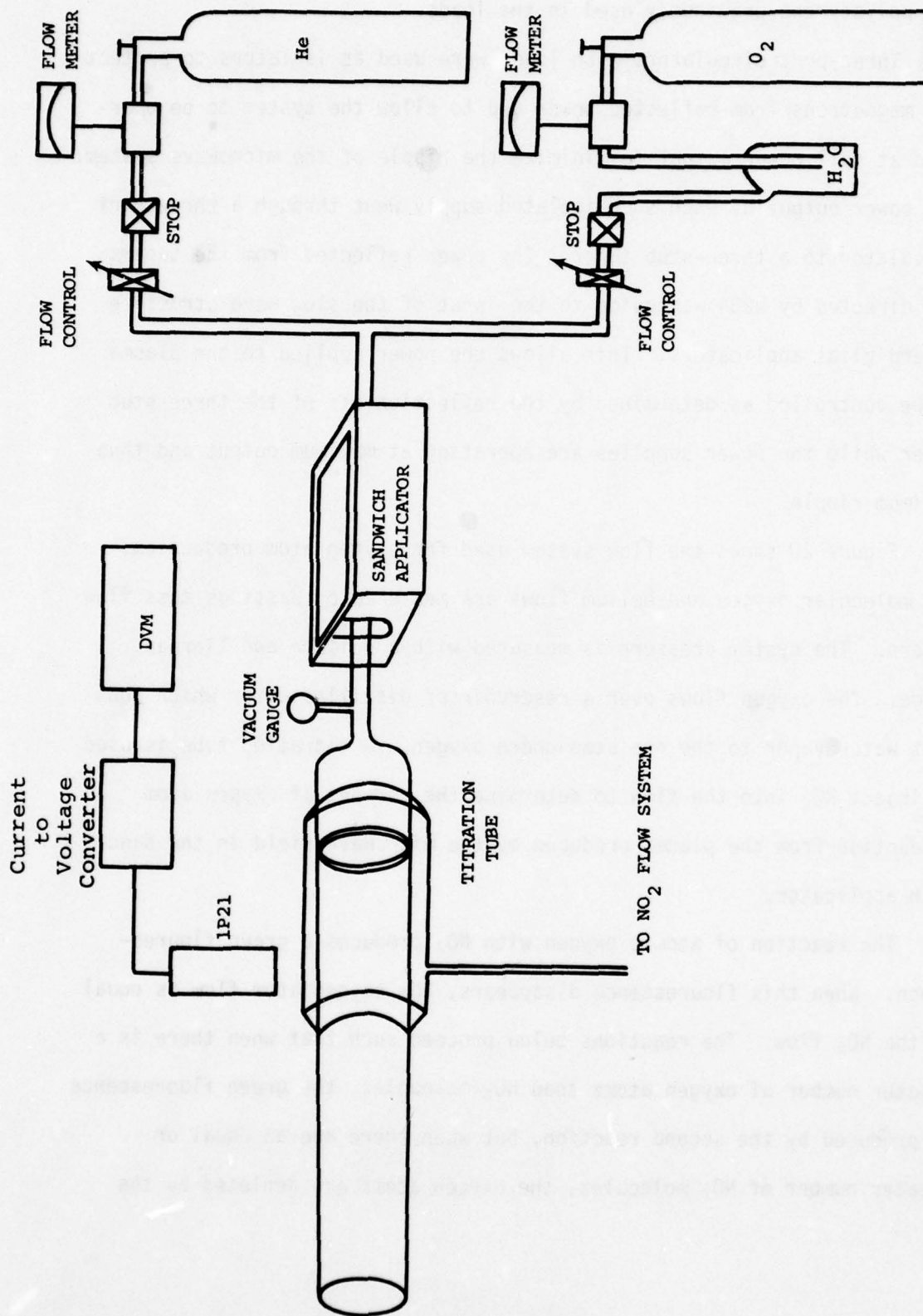
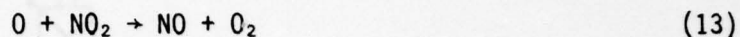


FIGURE 20 - OXYGEN FLOW SYSTEM

first reaction.



Because reaction (13) is so much faster than reaction (14) the NO_2 flow rate which quenches the fluorescence is equal to the oxygen atom flow rate.

The measurement of the NO_2 flow rate requires careful consideration. A Hastings type of mass flow meter is not suitable for this measurement, since gaseous NO_2 exists in an equilibrium mixture of $\text{N}_2\text{O}_4 \rightleftharpoons 2\text{NO}_2$ (for simplicity hereafter referred to as the NO_2 system). The percent of NO_2 in the equilibrium mixture depends on temperature and pressure. The principle of the operation of a Hastings type of mass flow meter is that it heats the flowing gas and the corresponding temperature change, dependent on the specific heat of the gas, is directly proportional to the flow rate. However, the specific heats of N_2O_4 and NO_2 are different, and if the mixture of N_2O_4 and NO_2 is heated, the percent of dissociation of N_2O_4 changes, and the specific heat of the equilibrium mixture changes. Therefore, the use of any mass flow meter requiring heat transfer is precluded since the specific heat of the mixture is strongly dependent on the NO_2 system equilibrium, which is temperature sensitive.

The titration of NO_2 was achieved by the method shown in Figure 21. The temperature of the water bath was maintained constant within 2°C for temperatures between 18 and 25°C by means of a capacitance type sensor which detects the column height in a mercury thermometer and controls

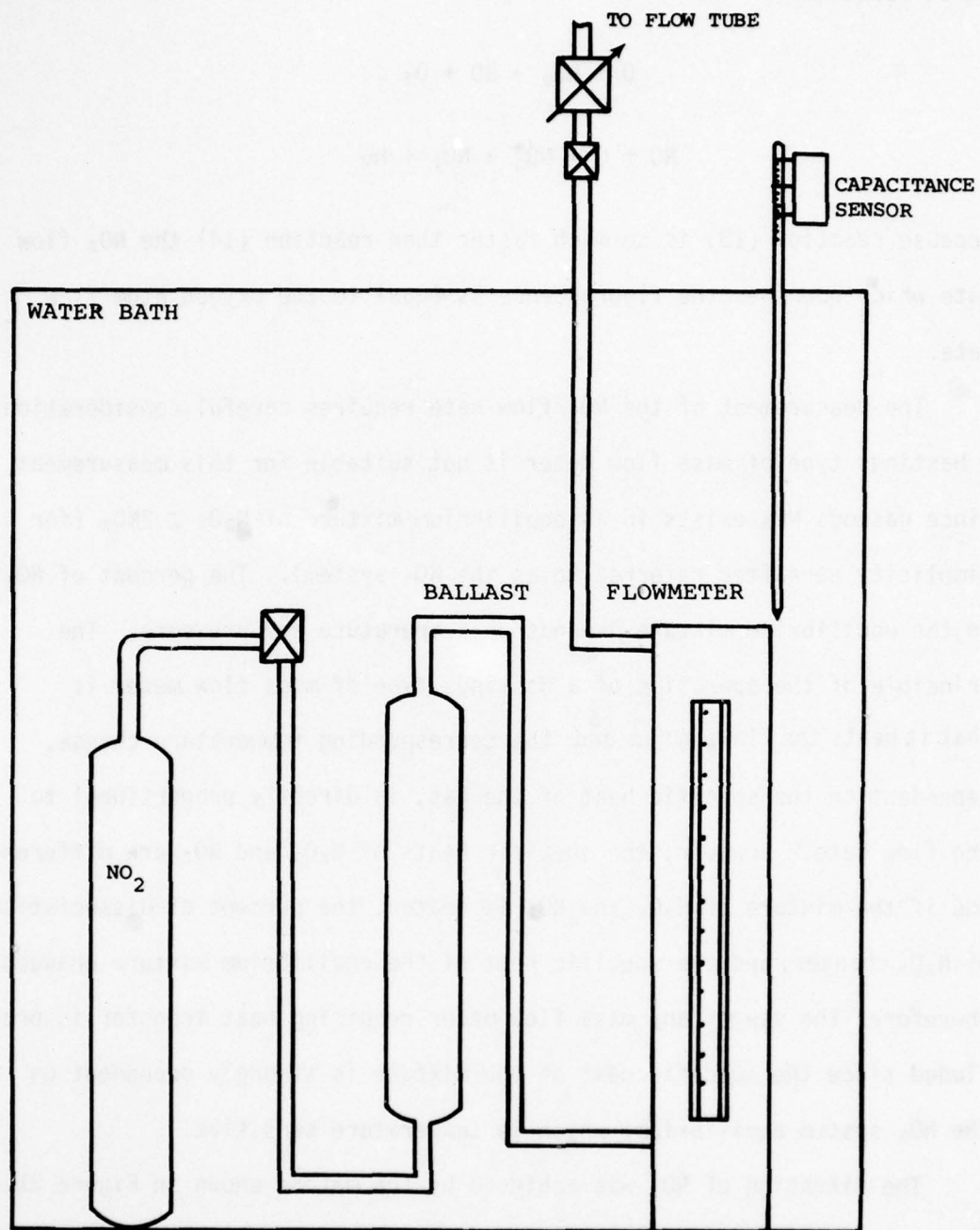


FIGURE 21 - NO_2 TITRATION SYSTEM

the power to four chromalox heaters. The NO_2 flow was measured by a tapered variable area flow meter with a diameter ratio scale.

The NO_2 flow, W , is given by¹⁵

$$W = CB \sqrt{(\rho_f - \rho_{\text{NO}_2}) \rho_{\text{NO}_2}}, \quad (15)$$

where B is the size factor constant for the flowmeter, ρ_f is the density of the flowmeter float, ρ_{NO_2} is the density of the $\text{N}_2\text{O}_4 \rightleftharpoons 2\text{NO}_2$ equilibrium, and C is the flow coefficient. The flow coefficient is dependent on the hydraulic characteristics of the flowmeter and the fluid being measured, which is a function of the flowmeter geometry and a parameter called the viscous influence number, VIN , defined as¹⁵

$$\text{VIN} = A \sqrt{\frac{(\rho_f - \rho_{\text{NO}_2}) \rho_{\text{NO}_2}}{\mu_{\text{NO}_2}}} \quad (16)$$

where A is the size factor constant of the tube and μ_{NO_2} is the viscosity of the $\text{N}_2\text{O}_4 \rightleftharpoons 2\text{NO}_2$ equilibrium. The constants A and B are given for the flowmeters, and tables supplied by the manufacturer relate VIN to the flow coefficient, C , as a function of flowmeter reading.

Therefore, the diameter ratio scale of the tapered, variable area flowmeter¹⁶ can be calibrated in mass flow rate units if the viscosity and density of the flowing gas are known. Sufficient data for the NO_2 system exist to determine these parameters.

The density of the NO_2 system was obtained in the following manner. A flow system consisting of a cylinder containing liquid N_2O_4 connected to a ballast and flowmeter by stainless steel tubing was placed in a

constant temperature water bath (Figure 21). The boil off of the liquid N_2O_4 was used as the source of NO_2 . The temperature change of the liquid due to boiling was negligible due to the thermal stability produced by the water bath. The pressure drop in the tubing and across the flowmeter float was negligible, and the residence time for the gas in the tubing assured thermal equilibration with the bath.

If the fractional dissociation α , of the N_2O_4 boil off at equilibrium is known at temperature T , then the pressure measured, P , is given by

$$PV = n(1-\alpha)RT(1+\lambda_1P) + 2n\alpha RT(1+\lambda_2P) \quad (17)$$

where V is volume, n is the number of N_2O_4 molecules with no dissociation, R is the gas constant, λ_1 is the gas imperfection for N_2O_4 , and λ_2 is the gas imperfection for NO_2 . If we assume that λ_1 for NO_2 is the same as for CO_2 and that¹⁷

$$\lambda_1 = 2\lambda_2 = .01(294/T)^3 \text{ atm}^{-1}$$

then

$$PV = nRT(1 + \lambda_1P) + n\alpha RT. \quad (18)$$

Since $n = m/M$ where m is the mass of N_2O_4 with no dissociation and M is the molecular weight of N_2O_4 , then

$$P = mRT(1 + \alpha + \lambda_1P)/(MV) \quad (19)$$

so that the density, $\rho = m/V$, is given by

$$\rho = PM/[(1 + \alpha + \lambda_1 P)RT] \quad (20)$$

The vapor pressure, P of the NO_2 system as a function of temperature has been determined with more than sufficient accuracy in our range of temperature, $293^\circ\text{K} < T < 298^\circ\text{K}$, as

$$\text{Log}_{10} P(\text{atm}) = 6.03631 - 1798.54/(3.64 + T) \equiv \text{Log}_{10} h(T) \quad (21)$$

The equilibrium constant, K , of the NO_2 system is given by⁴

$$K = 4\alpha^2 P/(1 - \alpha^2) \quad (22)$$

Sets of very good measurements of the equilibrium constant have been made.^{19,20,21,22} This data is plotted in Figure 22. A least squares fit of this data gives an equation for K as a function of temperature, i.e.,

$$\text{Log}_{10} K(\text{atm}) = 9.3385 - 3041.9/T \equiv \text{Log}_{10} g(T) \quad (23)$$

The slope of this line gives a value for the heat of reaction of 58 kJ/mole. This is within 2% of the value given in the JANAF tables.

We can now determine the density of the N_2O_4 system as a function of temperature only. The substitution for P and α in Eq. 20 with Eqs. (21), (22) and (23) allows the density to be written as

$$\rho = \frac{h(T) \cdot M}{\left(1 + \{g(T)/[4h(T) + g(T)]\}^{1/2} + \lambda_1 h(T)\right) RT} \quad (24)$$

Several experimental measurements of the viscosity of the NO_2 system as a function of temperature and pressure have been performed.^{23,24,25}

Using this data and Eq. (24) to determine the viscosity and density of

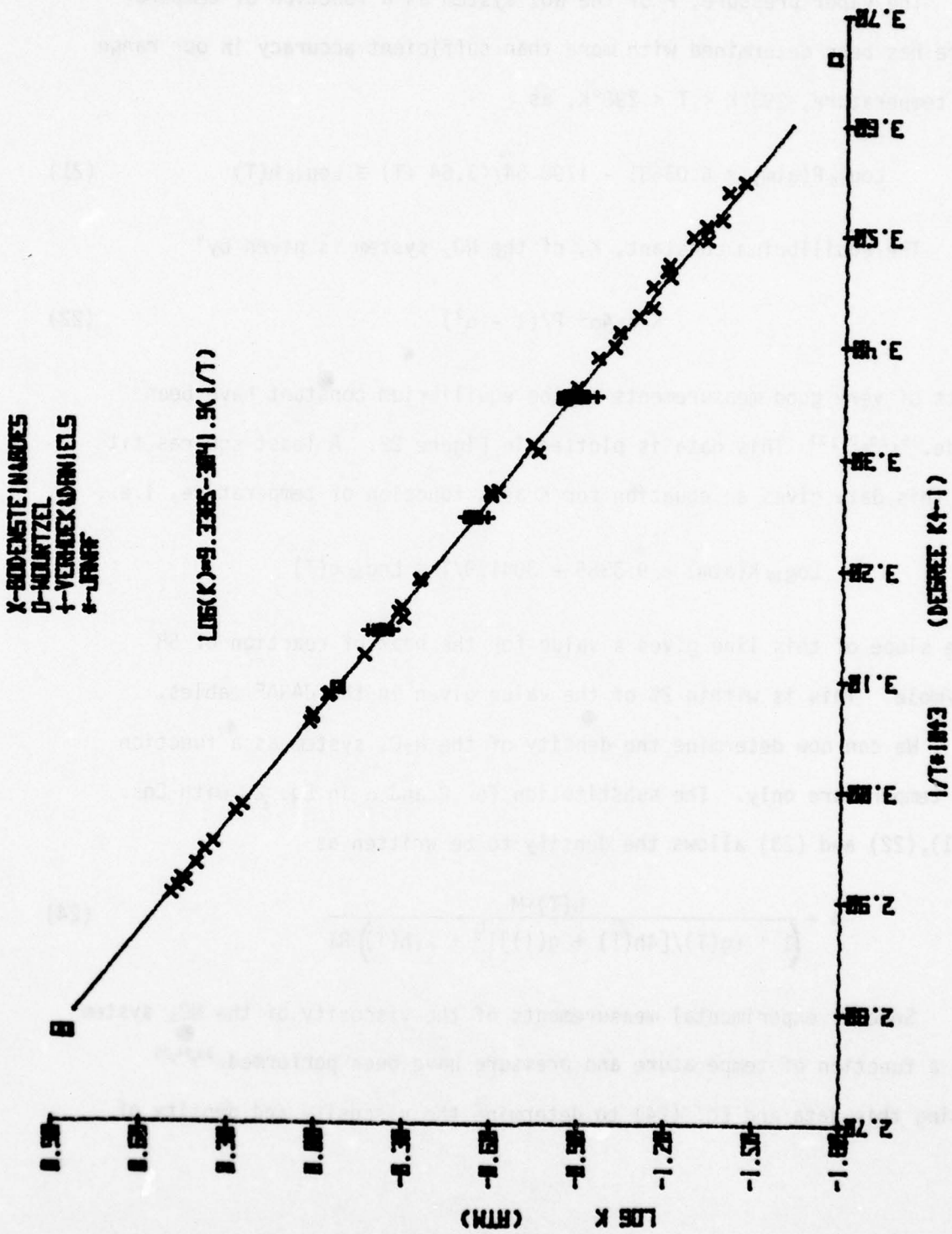


FIGURE 22 - LOG K VERSUS 1/T

the NO_2 system as a function of temperature, the NO_2 flow can be calculated from the known flowmeter tube characteristics.

To analyze possible sources of error in the calculations of the NO_2 flow, limits of error for each of the variables discussed were estimated. The corresponding errors in the NO_2 flow were calculated. Table I shows the results of this computer analysis.

To determine the accuracy of this method, the mass loss from a reservoir of liquid N_2O_4 during a timed run was measured. This loss was compared with program predictions for several flow rates. The measured error range was 4% at an NO_2 flow of 0.280 grams per minute to 20% at an NO_2 flow of 0.038 grams per minute. By determining the equilibrium density and viscosity from the method described, it is possible to determine the equilibrium flow rate and, thus, the equivalent NO_2 flow needed to extinguish the fluorescence of the reaction of Eq. (14).

The measurement of the point of extinction was facilitated by the use of a 1P21 photomultiplier tube. The NO_2 flow was increased slowly until the photomultiplier indicated the maximum optical output, I_{max} . At This point the NO_2 flow was then increased until the optical intensity dropped to a value of 2% of I_{max} . This point was considered extinction, and the NO_2 flow was equal to the oxygen atom flow. Tests with this method show that an NO_2 flow reproducibility of about 2% was achieved.

For the purpose of calculating the percent of oxygen atom production, Program I of the Appendix was written. Program II of the Appendix is a listing of the Block Data subprogram which contains the flow coefficient data for the viscous influence number as a function of flowmeter reading as supplied by the manufacturer.

TABLE 1

THE ACCURACY OF THE VARIABLES USED FOR THE NO₂ FLOW CALCULATION WAS ESTIMATED AND THE CORRESPONDING LIMIT OF ERROR IN THE FLOW MEASUREMENT IS SHOWN FOR THE FLOW RANGE DISCUSSED.

Variable	Estimated Limit of error	Flow Error at .038 g/min	Flow Error at .280 g/min
T	± 5%	2.0%	1.0%
K	± 5%	0.3%	0.2%
ρ	± 2%	2.0%	1.0%
P	± 2%	2.0%	1.0%
Viscosity	± 1%	1.0%	0.3%
Flowmeter reading	± 1% (Full scale)	11.0%	2.0%

Initial tests of the oxygen atom flow system were done without the water reservoir on the oxygen flow. It was found that the percent of oxygen atom production decreased with time. A possible explanation is that the heating of the quartz discharge tube by the plasma was cleaning the water from the walls of the discharge tube. Since the presence of water in the discharge increases the efficiency of dissociation of oxygen,²⁷ moist oxygen was used for testing. With .6% H₂O added to the oxygen, the oxygen atom production remained at a higher, more stable and reproducible rate than without the addition of water.

Results of the percent of oxygen atom production as a function of microwave power absorbed in the plasma at constant flow and pressure are shown in Figure 23. A maximum efficiency for the Gerling-Moore applicator system, in the longitudinal flow configuration, of 43 eV/atom was observed. This was in a 1 cm i.d. quartz tube with 330 watts absorbed in moist oxygen, 0.6% H₂O, at an oxygen flow of 450 sccm and velocity of 2700 cm/sec, and with a residence time in the 50 cm discharge of 20 msec.

A comparison of this work is that of McFarlane²⁸, Bosisio et al², and Mearns and Morris²⁷ is given in Table 2. The lower energy per atom required for short residence times indicates that a transverse flow across the present applicator would significantly increase its efficiency.

3. He-Ne LASER

The operation of a laser by microwave excitation eliminates the need for electrodes and thus a source of contamination to the laser medium. Because of the availability of a quartz tube He-Ne laser, this was chosen for initial testing. Figure 19 shows the microwave applicator system used to do microwave breakdown tests on a quartz tube

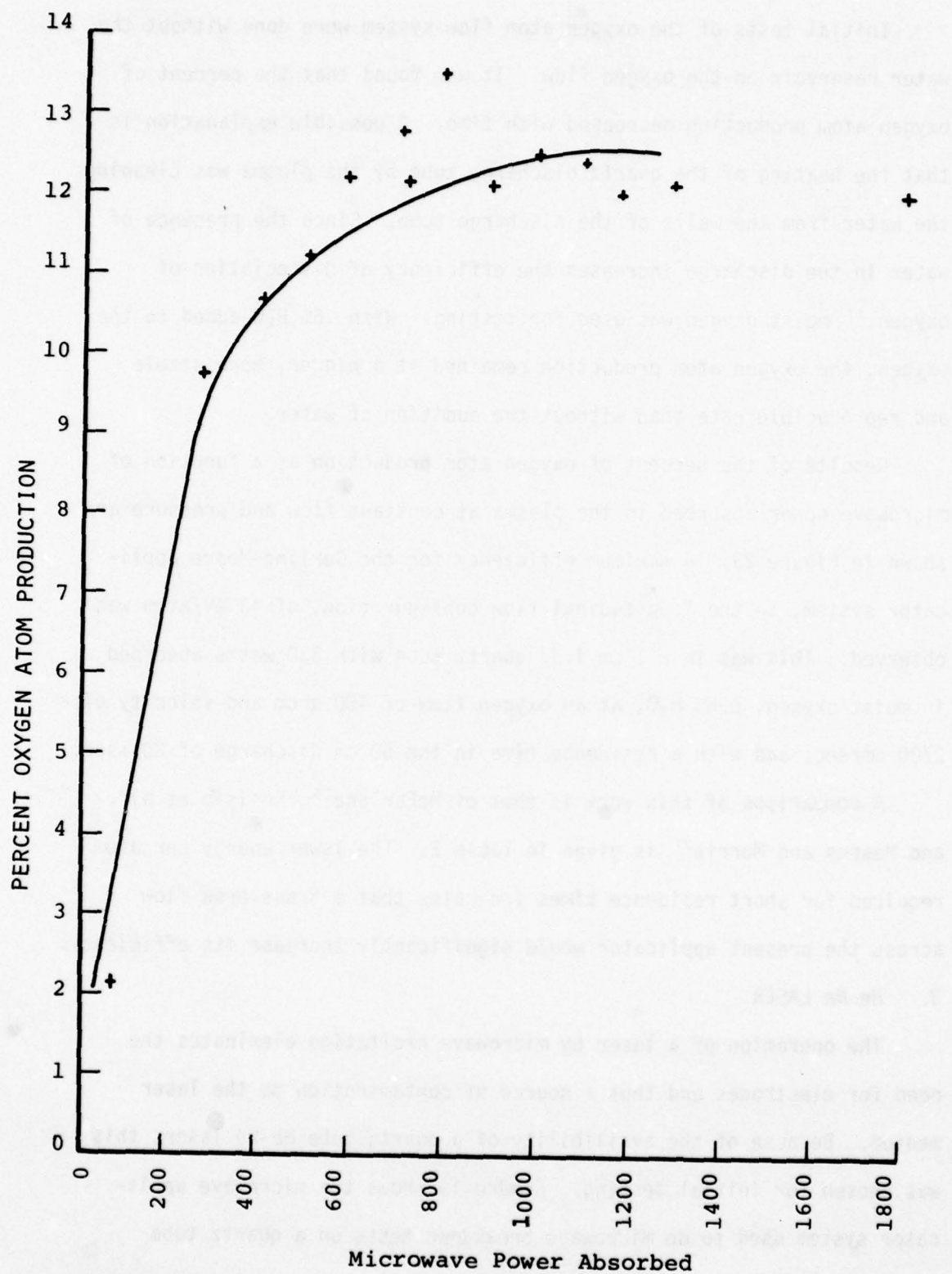


FIGURE 23 - PERCENT OF OXYGEN ATOM PRODUCTION VERSUS MICROWAVE POWER

TABLE 2

A COMPARISON OF THE OXYGEN ATOM PRODUCTION EFFICIENCY FOR VARIOUS METHODS OF MICROWAVE EXCITATION IS SHOWN.

	This Work	McFarlane	Bosisio et al.	Mearns Morris
Tube diameter (cm)	1	3	1.7	1
Flow (sccm)	450	940	1000	625
Pressure (Torr)	2.7	2.6	8	4
Moist O ₂	X			X
Quartz tube	X	X	X	
PTFE Tube				X
Orthophosphoric acid coating				X
Velocity (cm/s)	2,700	650	700	2,500
Residence time (ms)	20	35	130	1
Discharge length (cm)	50	22	90	2.5
Power absorbed (watts)	300	900-1,350	600	13
Efficiency (eV/atom)	43	35-46	80	3.5

He-Ne laser. The laser²⁹ (see Figure 24) was a 28 cm long, 6 mm o.d., 2 mm precision bore quartz tube, fitted with internal mirrors and electrodes for dc operation. The tube was filled to 1.9 torr with a mix of 87.5% He₄ and 12.5% Ne₂₀.

The tube was placed in the "sandwich" applicator and an attempt was made to obtain uniform ionization of the gas in the tube with microwaves only. The tube was tried in several positions with respect to the applicators' active surfaces, ending with the tube across the applicators with the output mirror touching the surface of the lower applicator. The tube was at an angle to the applicator such that the middle of the tube's cross section over the interdigital spacings was at a height of about 6 mm at the low power end of the lower applicator and about 12 mm at the power input end of the lower applicator. About 25 mm of the tube extended off the active surface at the low power end of the applicator and about 76 mm extended off the active surface at the power input end of the applicator. With about 800 watts of microwave power only transmitted to the applicator and about 100 watts absorbed by the tube, lasing action was achieved.

A Spectra Physics 401B power meter was used to measure the laser output. With the laser operating with dc power only, a variation in the laser power output indicated that alignment clamps to stabilize the laser tube were necessary.

With the output end of the laser mounted to the applicator with a teflon mount, and the reflector on a movable teflon mount connected to a Lansing mount, a current controlled dc discharge at 9mA and 3000V was used to align the laser. A maximum power of 2.5 mW was obtained. This was maintained for 30 minutes without adjustments. When the microwave

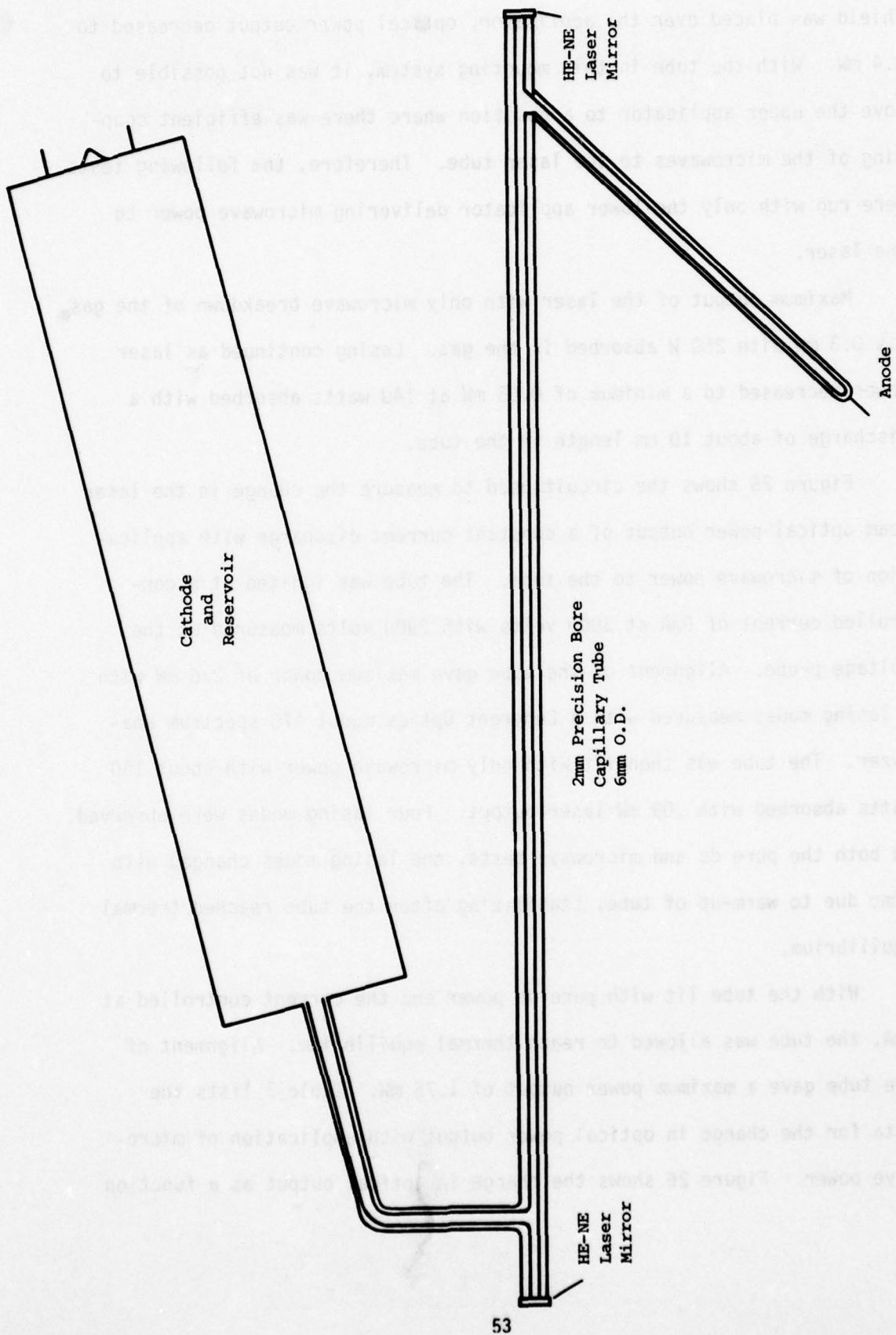


FIGURE 24 - QUARTZ TUBE HE - NE LASER

shield was placed over the applicator, optical power output decreased to 2.4 mW. With the tube in this mounting system, it was not possible to move the upper applicator to a position where there was efficient coupling of the microwaves to the laser tube. Therefore, the following tests were run with only the lower applicator delivering microwave power to the laser.

Maximum output of the laser with only microwave breakdown of the gas was 0.3 mW with 250 W absorbed in the gas. Lasing continued as laser power decreased to a minimum of 0.05 mW at 140 watts absorbed with a discharge of about 10 cm length in the tube.

Figure 25 shows the circuit used to measure the change in the laser beam optical power output of a constant current discharge with application of microwave power to the tube. The tube was ignited at a controlled current of 9mA at 3000 volts with 2900 volts measured at the voltage probe. Alignment of the tube gave maximum power of 2.6 mW with 7 lasing modes measured with a Coherent Optics model 470 spectrum analyzer. The tube was then lit with only microwave power with about 140 watts absorbed with .09 mW laser output. Four lasing modes were observed. In both the pure dc and microwave tests, the lasing modes changed with time due to warm-up of tube, stabilizing after the tube reached thermal equilibrium.

With the tube lit with pure dc power and the current controlled at 5mA, the tube was allowed to reach thermal equilibrium. Alignment of the tube gave a maximum power output of 1.75 mW. Table 3 lists the data for the change in optical power output with application of microwave power. Figure 26 shows the change in optical output as a function

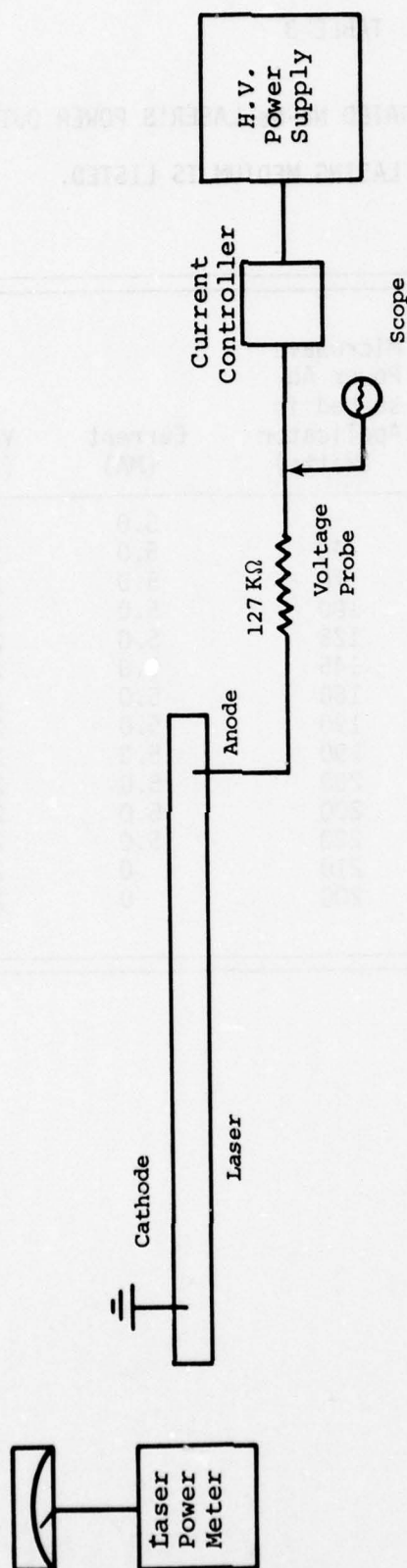


FIGURE 25 - INSTRUMENTATION FOR THE MEASUREMENT OF THE LASER BEAM OPTICAL OUTPUT POWER

TABLE 3

DATA ON THE CHANGE IN A DC OPERATED Ne-Ne LASER'S POWER OUTPUT AS MICRO-WAVE ENERGY IS ABSORBED IN THE LASING MEDIUM IS LISTED.

Microwave Power to Applicator (Watts)	Microwave Power Transmitted Through Applicator (Watts)	Microwave Power Ab- sorbed in Applicator (Watts)	Current (MA)	Voltage (Volts)	Laser Power (MW)
0	0	0	5.0	2475	1.75
50	10	40	5.0	2450	1.75
100	30	70	5.0	2425	1.80
150	50	100	5.0	2410	1.81
200	75	125	5.0	2400	1.84
250	105	145	5.0	2400	1.84
300	140	160	5.0	2375	1.88
350	160	190	5.0	2325	1.80
400	210	190	5.0	2250	1.75
450	250	200	5.0	2250	1.75
500	300	200	5.0	2200	1.80
550	330	220	5.0	2150	1.80
600	390	210	0	2900	0
800	600	200	0	2900	.175

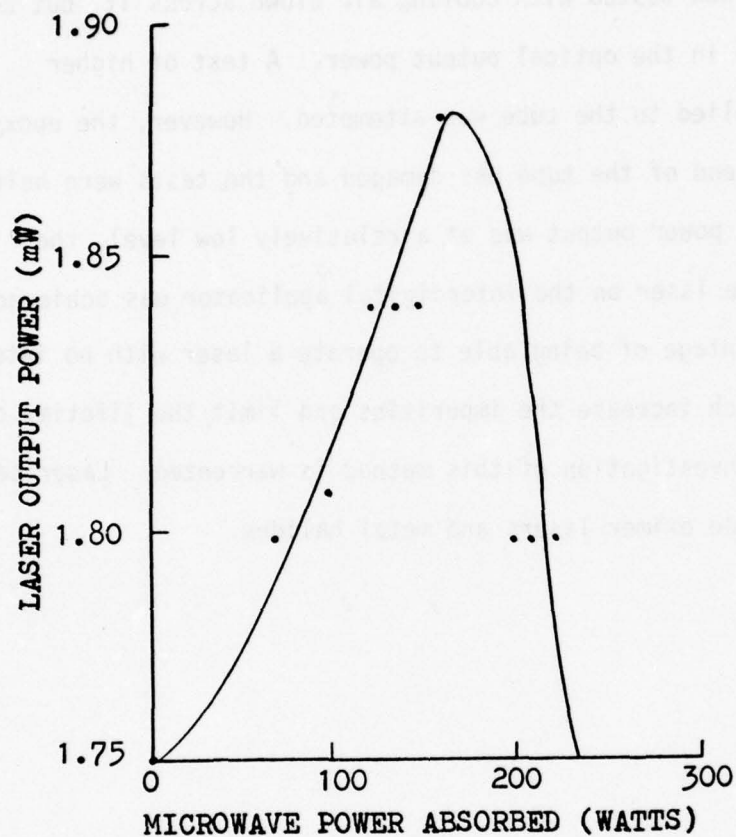


FIGURE 26. LASER BEAM OPTICAL POWER OUTPUT CHANGE
WITH RESPECT TO ABSORBED MICROWAVE POWER

of microwave power absorbed. This shows that the optical output power increases as microwave power increases up to about 160 watts and then decreases rapidly as the microwave power increases above this power level.

The tube was then tested with cooling air blown across it, but no difference was seen in the optical output power. A test of higher microwave power applied to the tube was attempted. However, the epoxy seal at the output end of the tube was damaged and the tests were halted.

Although laser power output was at a relatively low level, the operation of a He-Ne laser on the interdigital applicator was achieved. Because of the advantage of being able to operate a laser with no internal electrodes, which increase the impurities and limit the lifetime of the laser, further investigation of this method is warranted. Laser candidates would include eximer lasers and metal halides.

SECTION IV

TWIN ANTENNA IRRADIATOR SYSTEM

1. SYSTEM DESCRIPTION

The need for pulsed ultraviolet sources for photolysis has demanded emphasis on a new regime in pulsed light sources requiring higher temperatures and efficiencies for the production of electromagnetic radiation with wavelengths of 220 nm to 350 nm.³⁰ These new demands raise some questions as to whether the traditional xenon flash tubes would be the most effective source. It seems that other modes of excitation and other gases might be more suitable.

A recent development in cw ultraviolet sources using a 2.45 GHz microwave excited mercury arc tube has lead to efficiencies at least equivalent to the direct electric mercury arc with much longer lifetimes (3000 hours warranty) for the electrodeless tubes.³¹ An air cooled twin antenna irradiator in its commercial form deposits 120 watts per centimeter along a 25 cm, 8 mm i.d. tube. With a microwave power input of 3000 watts from 65% efficient magnetrons, the uv output in the region of interest was about 1000 watts, resulting in an overall efficiency somewhat better than 20%.³¹

Before the advent of the xenon flash tube which proved so superior in the visible spectrum, some work was done with pulsed electric discharge mercury tubes.³² These studies were done with cold tubes with an average temperature close to ambient. The tubes contained an excess of condensed mercury in a few torr of argon. When excited with a high voltage pulse with a half-width of about 3 μ sec at a one megawatt power

level, a corresponding width for the light pulse was produced with an output of 30 lumens per watt and thus an efficiency of up to one-half that of the cw irradiator produced light.

For these reasons a feasibility test on the pulsed ultraviolet production from microwave excited plasmas was undertaken. As a starting point the commercially available mercury filled tubes were tested with the twin antenna irradiator.

Initially this system was operated with a cw microwave input at both slotted antennas to ascertain the cooling and tuning required for operation. The microwave system used for cw testing is shown in Figure 27. Two 2.5 kW magnetrons fed power to the irradiator. Circulators with water cooled dummy loads protected the magnetrons from reflected power. The E-H tuner and the 3-stub tuners were used to produce the correct coupling and thus eliminate hot spots in the quartz of the mercury plasma tube. The plasma tubes were mounted in the irradiator inside a quartz cylinder through which cooling air was passed. A 1-1/2 horsepower Rotron blower provided cooling air for the discharge tube. The system was housed in a screen room to afford protection from microwave radiation leakage. A Holaday radiation monitor was used as an interlock in the system to prevent operation when microwave leakage exceeded a preset level, (0.01 mW/cm² to 1 mW/cm²).

The output of the discharge tube was measured outside the screen room (Figure 28). The ultraviolet radiation passed through a 10 db quartz neutral density filter and a waveguide below cutoff which was mounted through the screen room wall. Outside the screen room, a 1P28

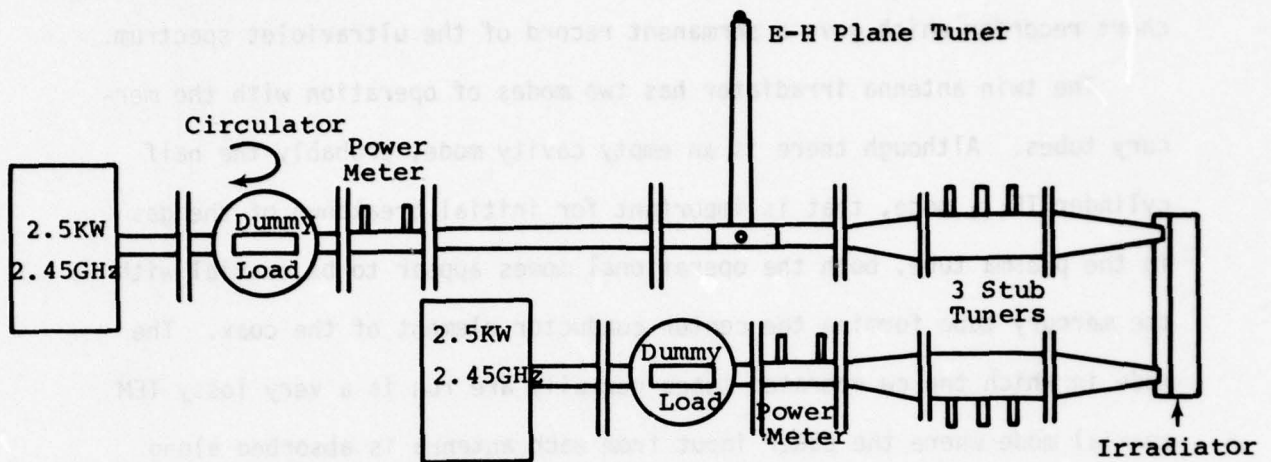


FIGURE 27. TWIN ANTENNA IRRADIATOR SYSTEM

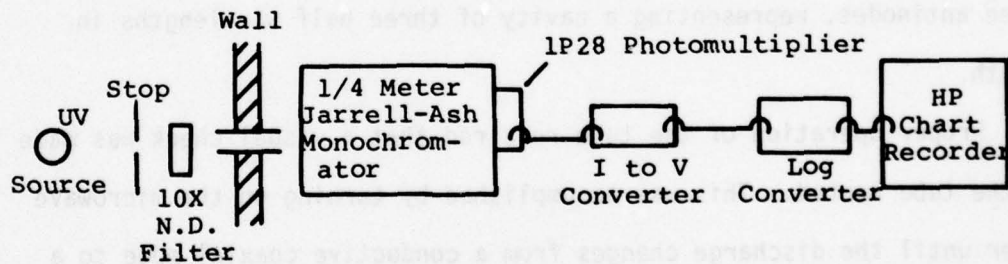


FIGURE 28. INSTRUMENTATION FOR CW-UV SPECTRAL MEASUREMENTS

photomultiplier at 900V with a 1/4 meter Jarrell-Ash monochromator was used to examine the ultraviolet output. The signal from the photomultiplier was amplified by a current to voltage converter with a gain range of 10^6 to 10^{12} . This output was recorded on a Hewlett Packard 7004B chart recorder which gave a permanent record of the ultraviolet spectrum.

The twin antenna irradiator has two modes of operation with the mercury tubes. Although there is an empty cavity mode, probably the half cylinder TE_{111} mode, that is important for initial breakdown of the gas in the plasma tube, both the operational modes appear to be coaxial with the mercury tube forming the center conductor element of the coax. The mode in which the cw operated tubes normally are run is a very lossy TEM coaxial mode where the power input from each antenna is absorbed along the discharge tube in an e-folding length of about half the cavity length. In the other mode of operation a coaxial cavity is formed, with the mercury plasma as a much less lossy effective center conductor, providing the usual standing wave coaxial mode. In this case there are three antinodes, representing a cavity of three half wavelengths in length.

Proper operation of the tube required that a visual check was made as the tube heated. This was accomplished by turning on the microwave power until the discharge changes from a conductive coaxial mode to a lossy coaxial mode. At this time, the cooling air was turned on. After the tube was operated in this mode for a few seconds, the microwave power was switched off a visual check for "red spots" on the quartz tube was made. If a hot spot was present, the cooling air flow and the micro-

wave coupling were changed until the spot was no longer observed. Once proper coupling and cooling were established the tube would run reproducibly without hot spots. Figure 29 shows a typical spectrum taken at 960 watts cw. Sample spectra were recorded for a number of conditions to have available for comparison studies and to compare with the efficiencies reported for the twin antenna irradiator. In the lossy coaxial mode with input powers up to 1200 watts the coupling was about 90% efficient. The spectra showed increasing band intensities in the 220 to 235 nm and 254 to 270 nm bands with increasing power and spectral efficiencies similar to those reported by Fusion Systems.³¹ Comparing these to standard direct electric mercury arc lamps, the temperatures at the center were about 7500°K; the electric fields were about 60 volts per centimeter; and the electron densities were about $10^{15}/\text{cc}$.³³

In the conductive coaxial mode the spectral efficiency was about 50% or higher, although the microwave power coupling was reduced to the order of 50 to 75%. This mode required considerably more tube cooling to operate.

2. PULSED ULTRAVIOLET MEASUREMENTS

The investigation of pulsed mercury discharges was undertaken next. The cw microwave power meters were calibrated for pulsed work. The outputs of the power meters were monitored on a Tektronix scope and a calibration for pulsed powers up to 4500 W was accomplished.

The system used for pulsed work is shown in Figure 30. The power combiner was tuned with the Gerling-Moore cw system and the Epsco pulse unit-2. The microwave pulse generators were triggered by a HP3310A

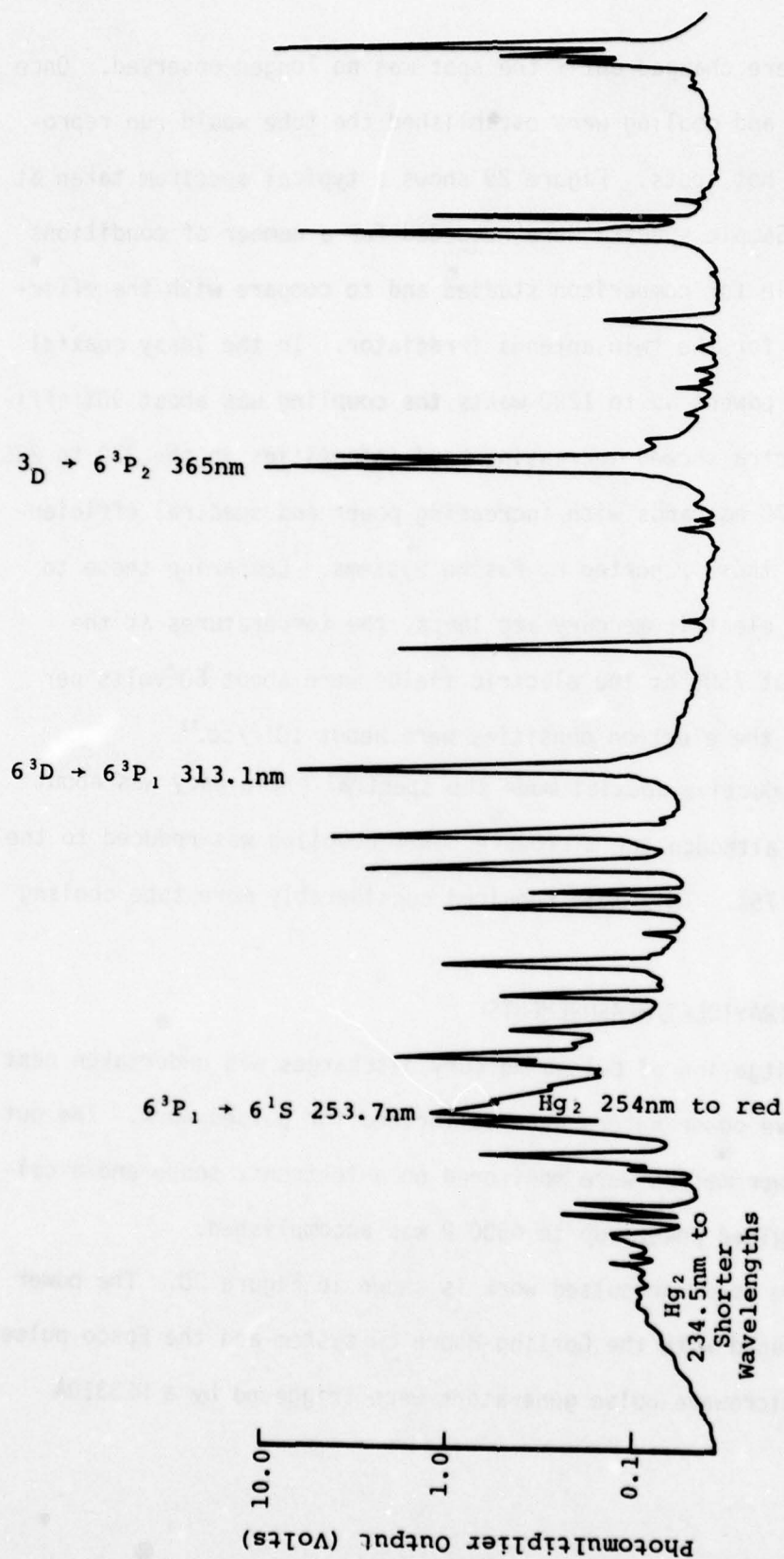


FIGURE 29. MERCURY SPECTRUM OF 930 WATT CW DISCHARGE

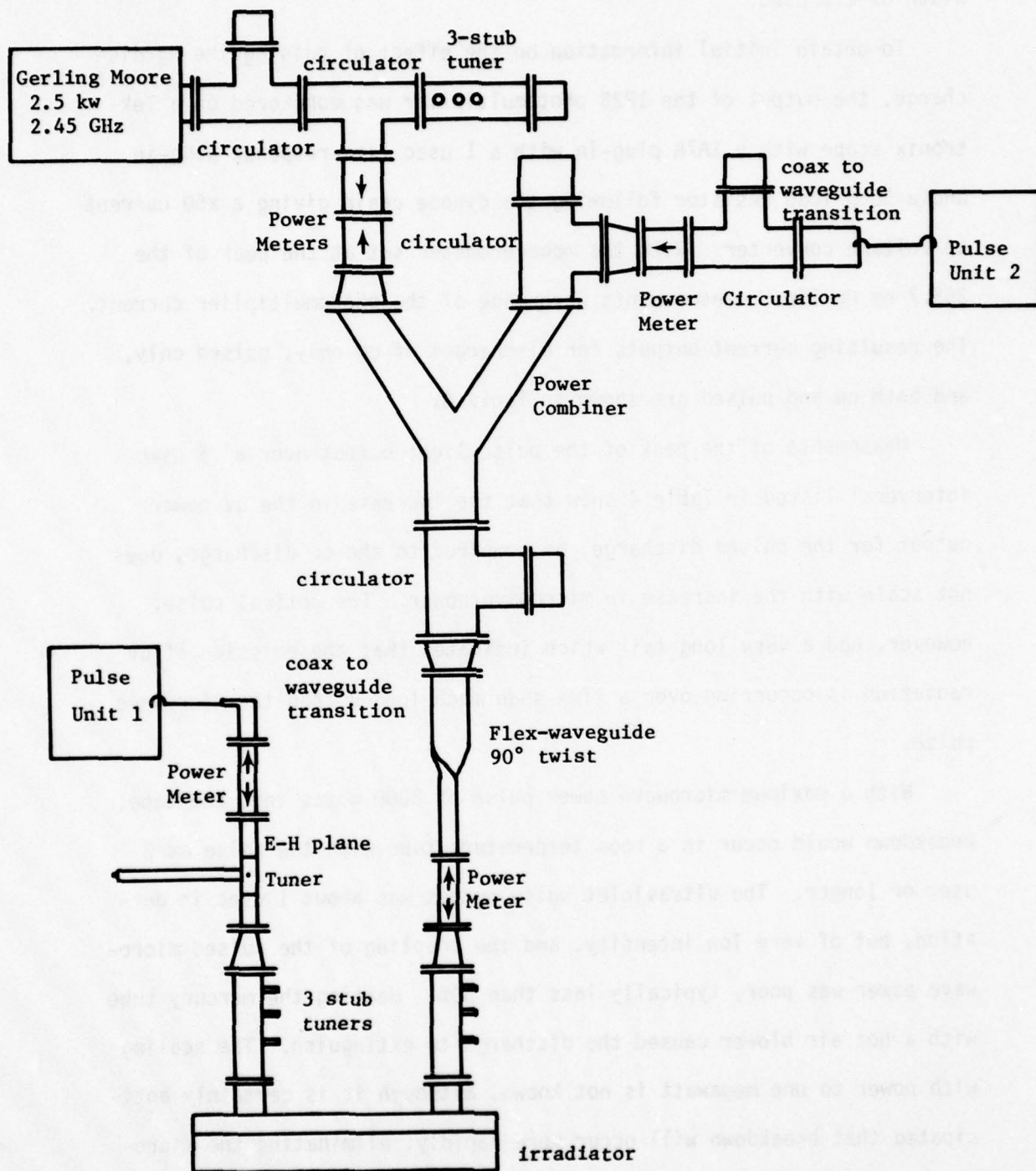


FIGURE 30. INSTRUMENTATION FOR PULSED MICROWAVE APPLICATION TO THE TWIN ANTENNA IRRADIATOR

function generator at 100Hz and were typically set for a microwave pulse width of 2.6 μ sec.

To obtain initial information on the effect of pulsing the Hg discharge, the output of the 1P28 photomultiplier was monitored on a Tektronix scope with a 1A7A plug-in with a 1 μ sec time response plug-in and a 50 Ω load resistor following the dynode chain giving a x50 current to voltage converter. With the monochrometer set at the peak of the 253.7 nm Hg line, measurements were made of the photomultiplier current. The resulting current outputs for discharges of cw only, pulsed only, and both cw and pulsed are shown in Table 4.

Measurements of the peak of the pulse light output over a .5 μ sec interval listed in Table 4 show that the increase in the uv power output for the pulsed discharge, as compared to the cw discharge, does not scale with the increase in microwave power. The optical pulse, however, had a very long tail which indicates that the emission of uv radiation is occurring over a time span much longer than the microwave pulse.

With a maximum microwave power pulse of 8000 watts into the tube, breakdown would occur in a room temperature tube with the pulse at 2 μ sec or longer. The ultraviolet pulse output was about 1 μ sec in duration, but of very low intensity, and the coupling of the pulsed microwave power was poor, typically less than 50%. Heating the mercury tube with a hot air blower caused the discharge to extinguish. The scaling with power to one megawatt is not known, although it is certainly anticipated that breakdown will occur more rapidly, eliminating the microsecond delay, and that higher pressures could be reached without extin-

TABLE 4

A COMPARISON OF THE UV OUTPUT FROM A MERCURY DISCHARGE WHEN OPERATED
CW AND PULSED.

Power	1P28 Output	uv output pulse width at half max. with 2.6 μ sec. micro- wave pulse
cw 110w	1×10^{-6} amp.	
pulsed 5500w	1.6×10^{-6} amp. max.	1.5 μ sec.
cw 110w + pulsed 5500w	1.1×10^{-5} amp. Max.	2.5 μ sec.

guishing the discharge.

To operate with the plasma at higher pressures, it was necessary to maintain a cw microwave power level sufficient to heat the mercury in the plasma tube to the temperature needed to produce the desired pressure. The first attempt was with the cw microwave power applied at only one antenna and the pulsed microwave power continuing to be applied at both antennas. With this arrangement, however, the sustainer discharge was nonuniform, and the tube was not heated at one end, resulting in the pressure of the mercury being controlled by the cold end of the tube. Since only one power combiner was available, the cw microwave power was fed into both antennas with equal input powers, and the pulsed power was applied to only one antenna. In Figure 30 pulse unit-1 was replaced with a cw microwave power generator.

In order to give some independent control of the mercury pressure at low cw microwave sustainer powers, a blower was used with a variable heating element allowing control of the temperature of the air blown over the plasma tube. At higher cw microwave sustainer powers, some control of the temperature of the plasma tube was possible by changing the rate of flow of the cooling air.

Spectral measurements of the ultraviolet output were made. However, use of the cw sustainer system complicated the task of making time resolved spectral measurements since the ultraviolet pulse signal was now riding on the cw sustainer background signal. To obtain time resolved spectra, the experimental arrangement shown in Figure 31 was used. The pulse generator was set at a frequency of 200 Hz. This pulse was used to trigger the PAR boxcar and the Tektronix 547 scope

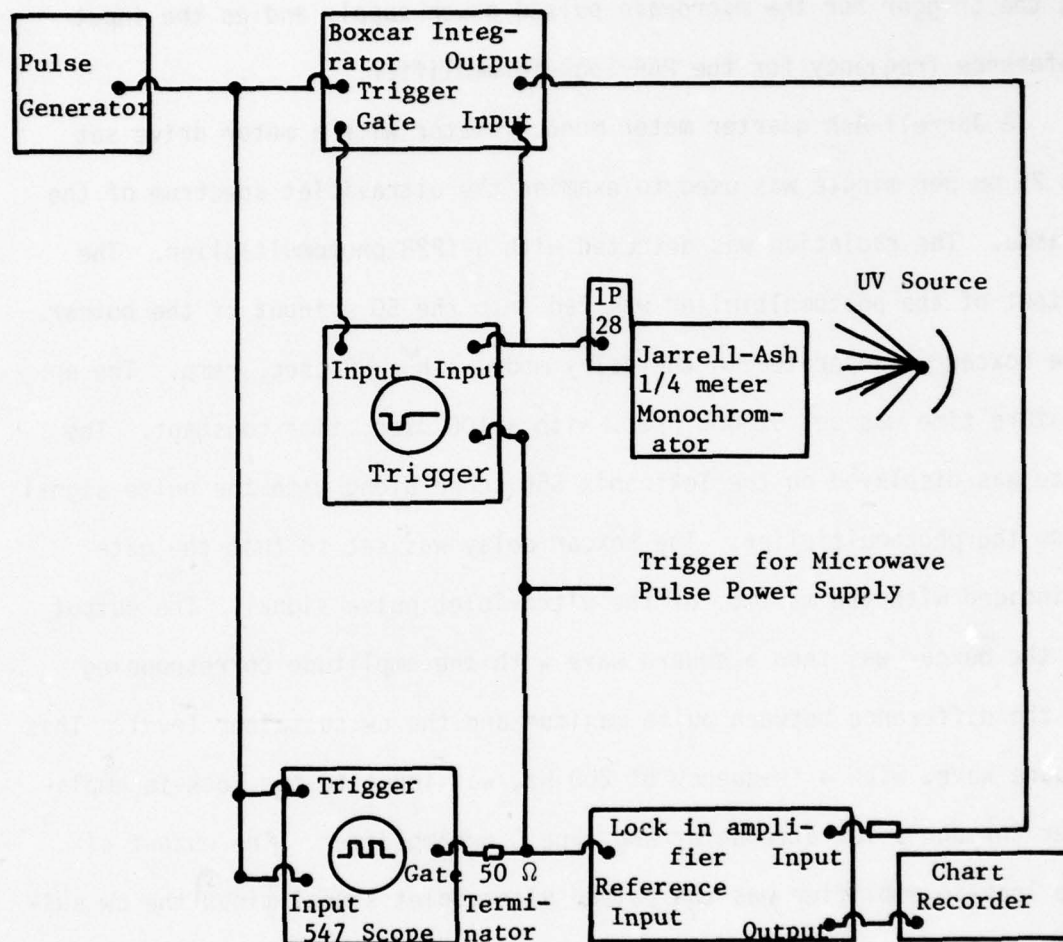


FIGURE 31. INSTRUMENTATION FOR PULSED UV

and was the input of the 547 scope. Two pulses were displayed on the scope, thus giving the gate output of the scope a frequency of 100 Hz, or half the input frequency. The gate output of the 547 scope was used as the trigger for the microwave pulsed-power supply and as the input reference frequency for the PAR lock-in amplifier.

A Jarrell-Ash quarter meter monochromator with a motor drive set at 25 nm per minute was used to examine the ultraviolet spectrum of the plasma. The radiation was detected with a 1P28 photomultiplier. The output of the photomultiplier was fed into the 50 Ω input of the boxcar. The boxcar was operated in the delay mode with a 50 μ sec. ramp. The aperture time was set at 0.5 μ sec. with a 100 μ sec. time constant. The gate was displayed on the Tektronix 556 scope along with the pulse signal from the photomultiplier. The boxcar delay was set so that the gate coincided with the maximum of the ultraviolet pulse signal. The output of the boxcar was then a square wave with the amplitude corresponding to the difference between pulse maximum and the cw sustainer level. This square wave, with a frequency of 200 Hz, was input to the lock-in amplifier through a 10x attenuator and type C preamplifier. The output of the lock-in amplifier was the pulsed ultraviolet signal minus the cw sustainer ultraviolet signal. A record of this spectral output was made on a Hewlett Packard chart recorder.

A series of spectra was taken under various conditions. First the cw sustainer discharge was operated in the conductive coaxial mode at low powers and at temperatures near room temperature. Then the cw sustainer discharge was operated in the lossy coaxial mode at low powers and exit air temperatures around 150°C. Finally the cw sustainer was

operated at higher powers in the lossy coaxial mode with exit air temperatures of about 210°C. For all these conditions, the pulsed microwave power was 3000 ± 200 watts with pulse lengths of 1, 2 and 4 μsec .

The relative intensity of the spectral lines was determined in the following manner. The spectral efficiency of the 3000 blaze grating of the Jarrell-Ash quarter meter monochromator was multiplied by the spectral sensitivity of the 1P28 photomultiplier tube giving the combined instrument sensitivity for the spectral region of interest. The normalized instrument sensitivity as a function of wavelength is shown in Figure 32. The relative intensity was determined by measuring the area under the lines of the raw spectra and multiplying this area by the relative instrument sensitivity factor.

Typical raw spectra are shown in Figure 33 and 34. For both of these spectra the microwave sustainer power was 200 watts and the microwave pulse was 4 μsec . long. However, the spectrum in Figure 33 was from a discharge in the lossy coaxial mode where the power coupling to the plasma was better than 90%, while the spectrum in Figure 34 was from a discharge in the conductive coaxial mode, where the power coupling to the plasma was only about 50%. The dominant feature of the spectrum in Figure 34 is the 253.7 nm mercury line while the spectrum in Figure 33 shows the 254 nm to red molecular mercury continuum in the spectral output. The emergence of the continuum and the decrease in the intensity of the 253.7 nm line, due to resonance trapping, indicate that the plasma was at a higher pressure when the discharge was operated in the lossy coaxial mode.

The relative spectral intensity of the 220 to 350 nm region is

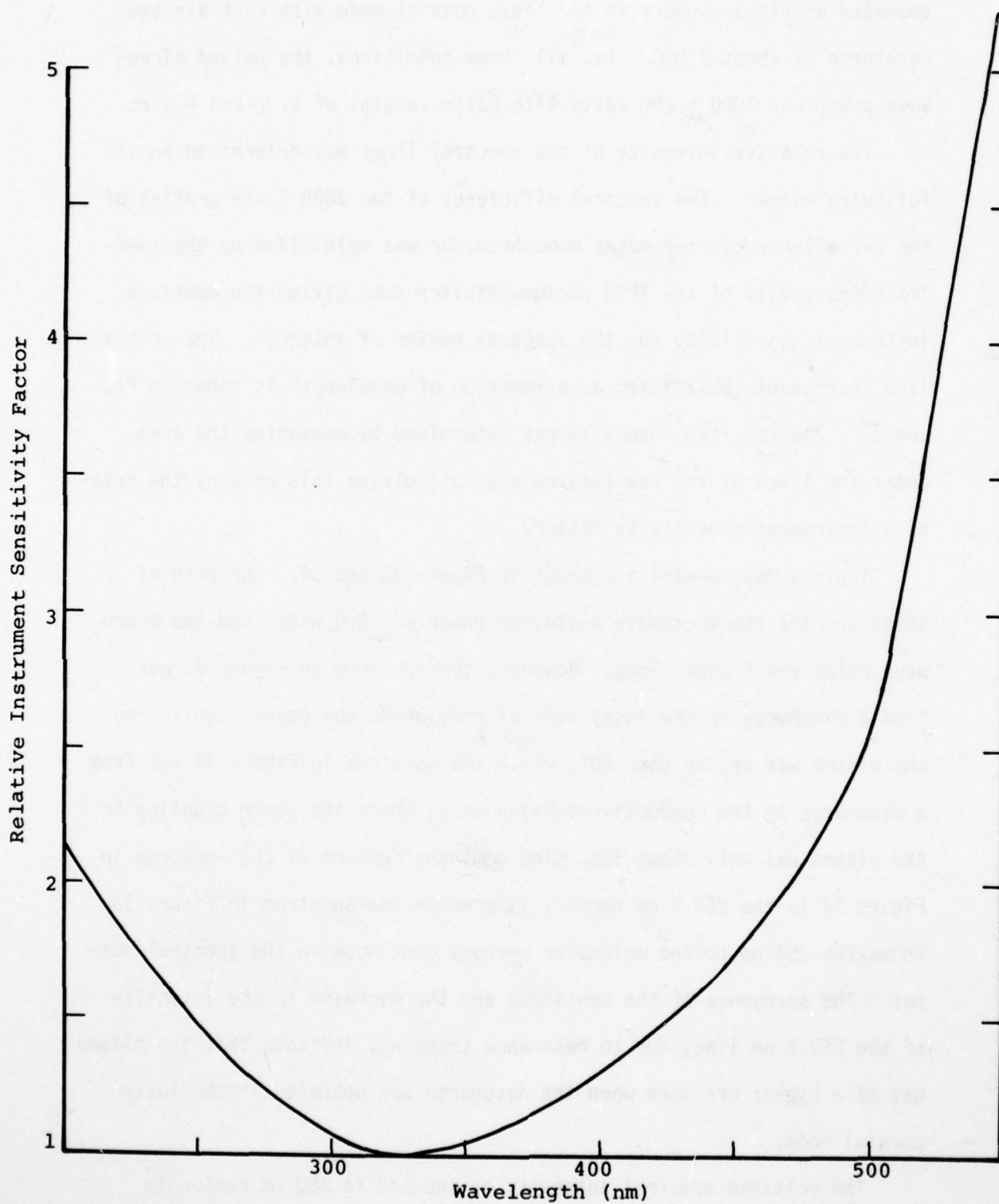


FIGURE 32. RELATIVE INSTRUMENT SENSITIVITY FACTOR AS A FUNCTION OF WAVELENGTH

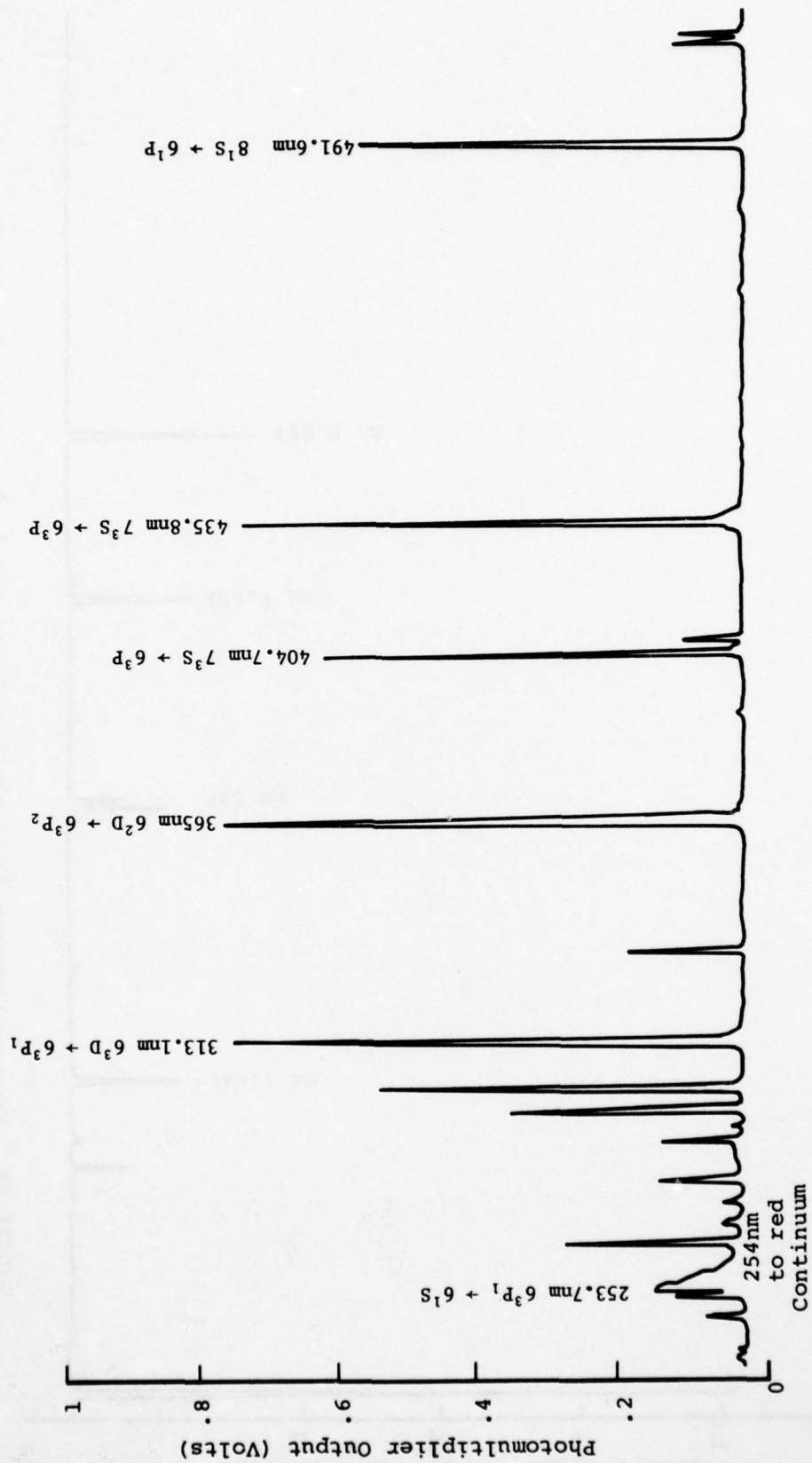


FIGURE 33. MERCURY SPECTRUM FROM 200 WATT DISCHARGE IN LOSSY COAXIAL MODE

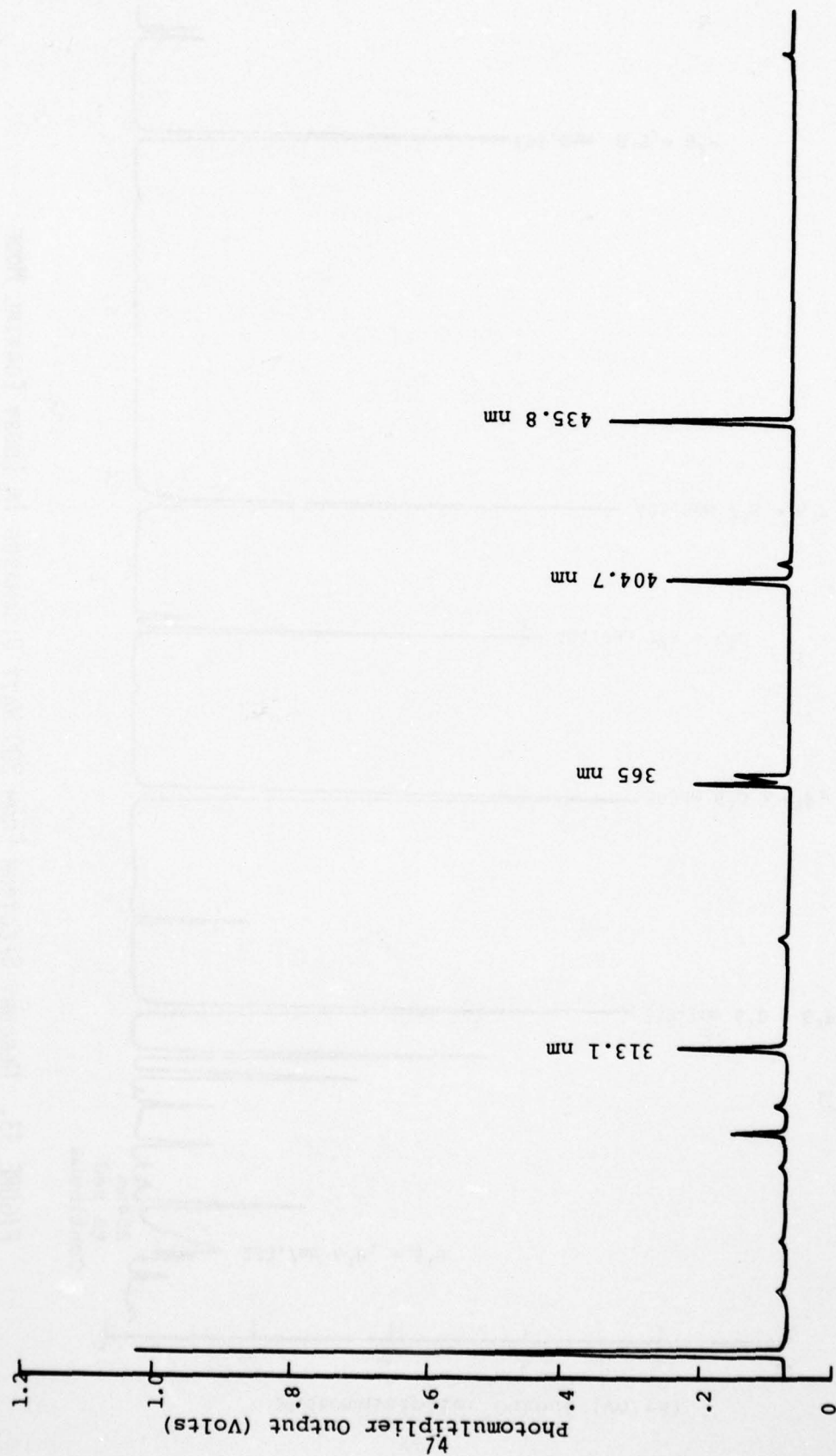


FIGURE 34. MERCURY SPECTRUM FROM 100 WATT DISCHARGE IN CONDUCTIVE COAXIAL MODE

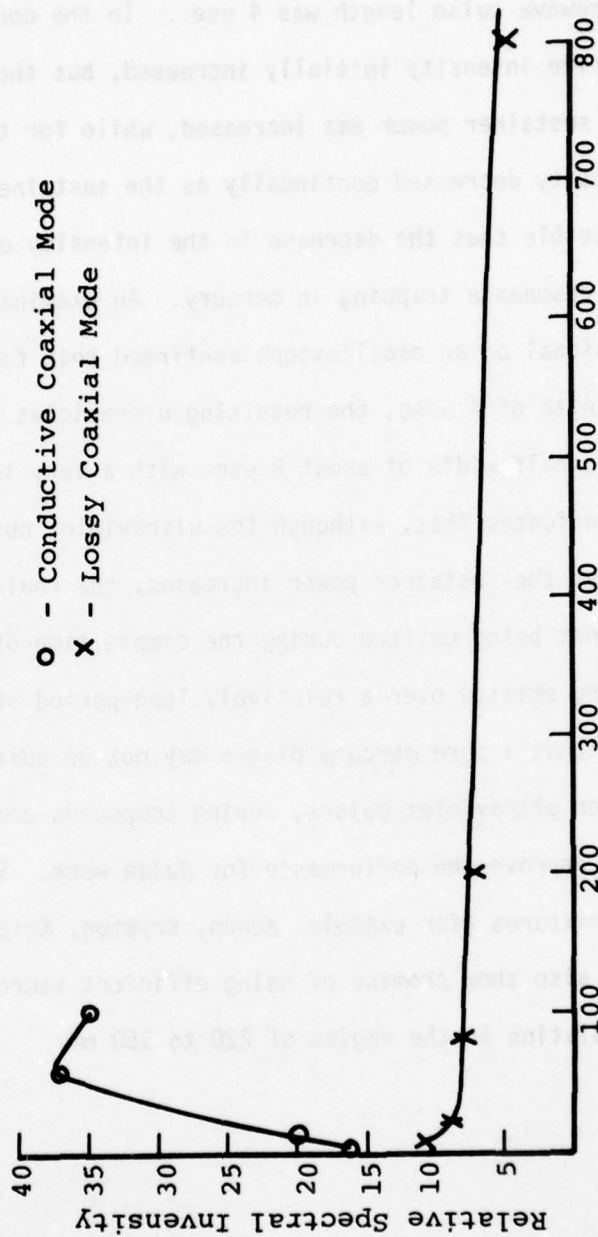


FIGURE 35. THE RELATIVE SPECTRAL INTENSITY OF THE 220NM TO 350NM RADIATION AS A FUNCTION OF MICROWAVE SUSTAINER POWER FOR TWO MODES OF TUBE OPERATION.

plotted as a function of microwave sustainer power in Figure 35. For the upper plot, the discharge was in the conductive coaxial mode, while for the lower plot the discharge was in the lossy coaxial mode. For both modes the microwave pulse length was 4 μ sec. In the conductive coaxial mode the relative intensity initially increased, but then started to decrease as the sustainer power was increased, while for the lossy coaxial mode the intensity decreased continually as the sustainer power increased.

It is possible that the decrease in the intensity of the pulse output is due to resonance trapping in mercury. An examination of the ultraviolet pulse signal on an oscilloscope confirmed that for a microwave power pulse length of 4 μ sec, the resulting ultraviolet pulse from the discharge had a half width of about 8 μ sec with a very long tail on the pulse. This indicates that, although the ultraviolet output may in fact be increasing as the sustainer power increases, the radiation from the discharge was not being emitted during the sample time of .5 μ sec but rather was being emitted over a relatively long period of time. While this indicates that a pure mercury plasma may not be suitable for generating high power ultraviolet pulses, doping compounds could be added to the mercury to improve the performance for pulse work. Several other gases and gas mixtures (for example: Xenon, Krypton, Krypton-Fluoride, Xenon-Arsenic) also show promise of being efficient sources of pulsed ultraviolet radiation in the region of 220 to 350 nm.

APPENDIX A - PROGRAM I

Fortran Program used to calculate the percentage of oxygen
atom production from a microwave discharge of oxygen

```

C *****ATMPRO*****
C
C
C
C THIS PROGRAM CALCULATES THE PERCENTAGE OF OXYGEN ATOM
C PRODUCTION FROM A MICROWAVE DISCHARGE OF OXYGEN.
C DETERMINATION OF OXYGEN ATOM PRODUCTION BY NO2 TITRATION
C MEASURED WITH A FISHER-PORTER VARIABLE AREA FLOW METER.
C INPUT PARAMETERS ARE: THE FLOW METER FLOAT MATERIAL:
C THE N2O4 EQUILIBRIUM TEMPERATURE: THE NO2 FLOW METER
C READING: AND THE OXYGEN FLOW RATE.
C
C LOAD WITH SUBPROGRAM VALUE (BLOCK DATA OF F-P COEFFICIENT DATA)
C
C VARIABLES
C R1,R2,R3= ALPHAMERIC RUN NUMBER
C IFLOAT= FLOAT MATERIAL
C EQFLO= NO2 FLOW METER READING 1<=EQFLO<=20
C DEGC= N2O4 EQUILIBRIUM TEMPERATURE IN DEGREES CELSIUS
C OXYGEN= OXYGEN FLOW RATE (SCCM)
C TEMP= EQUILIBRIUM TEMPERATURE IN DEGREES KELVIN
C K= EQUILIBRIUM CONSTANT
C P= PRESSURE (ATM)
C FLOAT= DENSITY OF FLOAT MATERIAL
C RHO= DENSITY OF EQUILIBRIUM FLOW
C MU= EQUILIBRIUM VISCOSITY
C VIN= VISCOUS INFLUENCE NUMBER
C COEF= FLOW COEFFICIENT
C W= NO2 FLOW RATE (MOLES/MIN)
C O2= OXYGEN FLOW RATE (MOLES/MIN)
C ATOM= PERCENT OF OXYGEN ATOM PRODUCTION
C
C PROGRAM-----ATMPRO
C REAL K,MIC(50),MU(50)
C INTEGER FSR
C DIMENSION R4(50),DEGC(50),EQFLO(50),ATOM(50),V(47,6)
C DIMENSION PRES(50),H2O(50),H2(50),W(50),O2(50)
C DIMENSION RHO(50),ALPHA(50),P(50),VIN(50),COEF(50),VC(2)
C COMMON R4,DEGC,EQFLO,ATOM,PRES,H2O,H2,W,O2,MIC/VALUE/V
C COMMON RHO,ALPHA,P,MU,VIN,COEF,VC
5 WRITE(8,10)
10 FORMAT(/,49H FLOAT MATERIAL ENTER: 1=SAPP ; 2=SS ; 3=TANT X)
READ (4,15) IFLOAT
15 FORMAT (I3)
WRITE (8,20)
20 FORMAT (/,34H FLOWMETER FULL SCALE READING = XX)
READ (4,21) FSR
21 FORMAT (I3)

```

Program I (cont'd)

```

25      WRITE(8,25)
      FORMAT(/,11H ENTER DATE)
      READ (4,30) R1,R2,R3
30      FORMAT (3A5)
      IF (IFLOAT-2) 45,40,35
35      FLOAT=16.6
      WRITE (8,36)
36      FORMAT (/,16X,15H TANTALUM FLOAT)
      GO TO 50
40      FLOAT=8.01
      WRITE (8,41)
41      FORMAT (/,16X,22H STAINLESS STEEL FLOAT)
      GO TO 50
45      FLOAT=3.98
      WRITE (8,46)
46      FORMAT (/,16X,15H SAPPHIRE FLOAT)
50      WRITE (8,51) FSR
51      FORMAT (/16X,21H FULL SCALE READING =,I3)
      DO 210 M=1,50
      WRITE (8,60)
60      FORMAT (17H ENTER RUN NUMBER)
      READ (4,65) R4(M)
65      FORMAT (3A5)
      WRITE (8,70)
70      FORMAT (/,30H NO2 FLOW METER READING = XX.X)
      READ (4,75) EQFLO(M)
75      FORMAT (F5.1)
      WRITE (8,80)
80      FORMAT (/,31H TEMPERATURE OF NO2 FLOW = XX.X)
      READ (4,85) DEGC(M)
85      FORMAT (F5.1)
      WRITE (8,90)
90      FORMAT (/,32H OXYGEN FLOW RATE (SCCM) = XXXX.)
      READ (4,95) OXYGEN
95      FORMAT (F6.0)
      WRITE (8,100)
100     FORMAT (/,28H SYSTEM PRESSURE = XX.X TORR)
      READ (4,105) PRES(M)
105     FORMAT (F5.1)
      WRITE (8,110)
110     FORMAT (/,25H PERCENT H2O ADDED = X.XX)
      READ (4,115) H2O(M)
115     FORMAT (F5.2)
      WRITE (8,120)
120     FORMAT (/,24H H2 PRESSURE = .XXX TORR)
      READ(4,125) H2(M)
125     FORMAT (F5.3)
      WRITE (8,130)
130     FORMAT (/,24H MICROWAVE POWER = XXXX.)
      READ (4,135) MIC(M)
135     FORMAT (F5.0)

```

Program I (cont'd)

```

C
CALCULATION OF VISCOUS FLOW NUMBER
C
140  TEMP=273.16+DEGC(M)
      K=10**((9.3385-3041.9/TEMP)
      P(M)=10**((6.03631-1798.54/(3.46+TEMP))
      ALPHA(M)=SQRT(K/(4.*P(M)+K))
      RHO(M)=P(M)*92.0116/((1+ALPHA(M)-.01*(294/TEMP)**3.*P(M))*8.207E
      1-02*TEMP)*1E-03
      T=TEMP-290.
      IF(P(M).LE.1) GO TO 150
      MU(M)=(128.+6*T-P(M))*1E-04
      GO TO 155
150  MU(M)=(127.+6*T*P(M))*1E-04
155  VIN(M)=1.43E+02/MU(M)*SQRT((FLOAT-RHO(M))*RHO(M))
C
CALCULATION OF FLOW COEFFICIENT
C
      IF(FSR.NE.20) GO TO 160
      LSR=1
      J=0
160  IF(FSR.NE.16.AND.FSR.NE.10) GO TO 165
      LSR=3
      J=(388-19*FSR)/6
165  IF(FSR.NE.12.AND.FSR.NE.8) GO TO 170
      LSR=2
      J=72-4*FSR
170  CONTINUE
      X=2.
      DO 175 L=FSR,8,-2
      J=J+1
      IF(EQFLO(M).GT.L) GO TO 185
175  CONTINUE
      X=1.
      DO 180 L=7,LSR,-1
      J=J+1
      IF(EQFLO(M).GT.L) GO TO 185
180  CONTINUE
      L=LSR
185  DO 190 JL=1,2
      IF(VIN(M).GE.V(J,6)/2.) VC(JL)=V(J,1)-(V(J,2)/VIN(M)**.25)
      IF(V(J,6)/2..GT.VIN(M).AND.VIN(M).GT.V(J,6)/5.) VC(JL)=
      1V(J,3)*VIN(M)-V(J,4)*VIN(M)**2.
      IF(VIN(M).LE.V(J,6)/5.) VC(JL)=V(J,5)*VIN(M)
      J=J-1
190  CONTINUE
      COEF(M)=VC(1)+(VC(2)-VC(1))*(EQFLO(M)-L)/X
C
CALCULATION OF NO2 FLOW (MOLES/MIN)
C
      W(M)=COEF(M)*13.6*SQRT((FLOAT-RHO(M))*RHO(M))/43.0058

```


Program I (cont'd)

```

C
CALCULATION OF % OXYGEN ATOMS
C
      O2(M)=OXYGEN/2.2414E+04
      ATOM(M)=W(M)/O2(M)/2.*100.
      ALPHA(M)=ALPHA(M)*100.
      WRITE (8,200)
200   FORMAT (/52H NEXT SET OF DATA TYPE 1 ; PRINT OUT RESULTS TYPE 9)
      READ (4,205) II
205   FORMAT (I2)
      IF (II.NE.1) GO TO 215
210   CONTINUE
C
C   PRINT OUT OF CALCULATIONS
C
215   DO 290 I=1,M
      IF (DEGC(I).GE.18..AND.DEGC(I).LE.25.) GO TO 225
      WRITE(8,220)
220   FORMAT (/,,/,/,/,/,26H TEMPERATURE OUT OF RANGE.)
      PAUSE 111111
225   IF (EQFLO(M).GE.1..AND.EQFLO(M).LE.FSR) GO TO 235
      WRITE (8,230)
230   FORMAT (/,,/,/,/,23H NO2 FLOW OUT OF RANGE.)
      PAUSE 222222
235   WRITE (8,240)R1,R2,R3,R4(I),DEGC(I),EQFLO(I),RHO(I),ALPHA(I),P(I),
      1MU(I),VIN(I),COEF(I)
240   FORMAT (////1X,3A5,6H RUN #,A5,/,23H TEMPERATURE NO2 FLOW =,F5.1
      1,17H DEGREES CELSIUS,/,25H NO2 FLOW METER READING =,F5.1
      2,/,22H EQUILIBRIUM DENSITY =,F8.5,10H GRAMS/CC,/,20H N2
      304 DISSOCIATION =,F5.1,3H %,/,23H EQUILIBRIUM PRESSURE =
      4,F5.2,5H ATM,/,24H EQUILIBRIUM VISCOSITY =,F7.4
      5,5H CPS,/,27H VISCOUS INFLUENCE NUMBER =,F7.1,/,19H FLOW C
      60EFFICIENT =,F8.5,/)
      WRITE (8,245) MIC(I),PRES(I),H2O(I),H2(I),W(I),O2(I),ATOM(I)
245   FORMAT (27H MICROWAVE POWER ABSORBED =,F5.0,7H WATTS,/,18
      1H SYSTEM PRESSURE =,F5.1,6H TORR,/,12H H2O ADDED =,F5.2,3
      2H %,/,17H HYDROGEN ADDED =,F5.3,6H TORR,/,11H NO2 FLOW =
      3,E10.3,11H MOLES/MIN,/,14H OXYGEN FLOW =,E10.3,11H MOLES/
      4MIN,/,25H OXYGEN ATOM PRODUCTION =,F6.2,3H %)
290   CONTINUE
      GO TO 5
      STOP 100
900   END

```

APPENDIX B - PROGRAM II

Fortran block data program of the coefficient relating the viscous influence number to the flow coefficients as a function of meter reading for 1/14 flowmeters.

```

C SUBPROGRAM VALUE
C THIS IS A BLOCK DATA PROGRAM WITH THE 282 VALUES OF THE
C COEFFICIENTS RELATING THE VISCOUS INFLUENCE NUMBERS TO THE
C FLOW COEFFICIENTS AS SUPPLIED BY F-P IN THEIR DATA FOR THE
C 1/16 FLOW METERS
C
C IF VIN>N'/2 THEN COEF=r-(s/VIN**.25)
C
C IF N'/5<VIN<N'/2 THEN COEF=p*VIN-q*VIN**2.
C
C IF VIN<N'/5. THEN COEF=m*VIN
C
C *****BLOCK DATA PROGRAM VALUE*****
C BLOCK DATA
C COMMON /VALUE/V(47,6)
C
C *****r VALUES*****
C
C DATA V/.81362,.74287,.67876,.54410,.46545,.36112,.28780,
C 2.25229,.18569,.16301,.17595,.11018,.078382,.029947,
C 6.60096,.52413,.43793,.37805,.24930,.22831,.21466,.22022,.21275,
C 6.21608,
C 2.47557,.36699,.31014,.31135,.29667,.28228,.26957,.19045,
C 2.062205,
C 1.46099,.35401,.32298,.28518,.29025,.22711,.054281,
C 8.33716,.29483,.28563,.26421,.18365,.13947,-.0063791,
C
C *****s VALUES*****
C
C 22.2764,2.1552,2.087,1.5882,1.4724,1.1222,.97585,.89942,
C 2.58263,.55367,.82733,.46438,.33802,.1067,
C 61.7849,1.605,1.3945,1.3289,.74196,.74353,.81306,1.0177,
C 61.12,1.329,
C 21.5568,1.1896,1.1642,1.3571,1.428,1.4794,1.5511,1.169,
C 2.41759,
C 11.8001,1.4555,1.4376,1.3568,1.595,1.3251,.29858,
C 81.2838,1.1922,1.335,1.3793,.9818,.87684,-.16534,
C
C *****p VALUES*****
C
C 2.99934E-3,.81696E-3,.65784E-3,.48743E-3,.3685E-3,.24217E-3,
C 2.1591E-3,.11767E-3,.84742E-4,.54929E-4,.34582E-4,.19397E-4,
C 2.10997E-4,.50301E-5,
C 6.65124E-3,.4786E-3,.35799E-3,.24261E-3,.13626E-3,.10342E-3,
C 6.7624E-4,.49784E-4,.29251E-4,.15887E-4,
C 2.35155E-3,.22603E-3,.13676E-3,.10143E-3,.63427E-4,.37904E-4,
C 2.21194E-4,.11301E-4,.3663E-5,
C 1.21169E-3,.10854E-3,.79426E-4,.49784E-4,.31501E-4,.17218E-4,
C 1.52796E-5,
C 8.11241E-3,.84971E-4,.57789E-4,.36613E-4,.20477E-4,.91884E-5,
C 8.41031E-5,

```

Program II (cont'd)

C
C
C

*****a VALUES*****

2.66907E-6,.50285E-6,.37619E-6,.22777E-6,.1665E-6,.81765E-7,
2.48143E-7,.30298E-7,.17728E-7,.85246E-8,.41785E-8,.16313E-8,
2.70274E-9,.33436E-9,
6.40193E-6,.25026E-6,.16694E-6,.93768E-7,.32294E-7,.22044E-7,
6.14863E-7,.75573E-8,.2947E-8,.80013E-9,
2.1543E-6,.71799E-7,.36512E-7,.24905E-7,.10028E-7,.34685E-8,
2.40656E-9,.2208E-9,.1785E-9,
1.69074E-7,.15768E-7,.1237E-7,.37652E-8,.23736E-8,.4124E-9,
1.30286E-9,
8.19801E-7,.1365E-7,.72708E-8,.34643E-8,.13702E-8,.42775E-9,
8.34593E-9,

C
C
C

*****m VALUES*****

2.81029E-3,.66958E-3,.53947E-3,.40811E-3,.30729E-3,.20805E-3,
2.1317E-3,.96599E-4,.69109E-4,.45654E-4,.28043E-4,.1671E-4,
2.86814E-5,.39285E-5,
6.52543E-3,.39656E-3,.28941E-3,.19369E-3,.11788E-3,.88083E-4,
6.63667E-4,.41426E-4,.25931E-4,.13251E-4,
2.29536E-3,.19607E-3,.11521E-3,.84184E-4,.5279E-4,.34165E-4,
2.2077E-4,.10842E-4,.31137E-5,
1.17951E-3,.10126E-3,.71209E-4,.47192E-4,.29326E-4,
1.1668E-4,.42818E-5,
8.96913E-4,.69712E-4,.471E-4,.30906E-4,.18219E-4,.82958E-5,
8.30893E-5,

C
C
C

*****N PRIME VALUES*****

21412.8,1465.4,1573.2,1741.1,1838.3,2086.7,2845.5,3477.8,
24409.3,5440.2,7825.,8236.8,16474.,16474.,
61565.,1639.1,2054.1,2608.3,2845.5,3477.8,4229.7,5529.7,
65634.,16474.,
21820.7,2086.7,2952.2,3462.2,5303.6,5390.6,5216.7,10401.,15389.,
12328.9,2310.2,3321.3,3443.,4583.2,6520.8,16474.,
83912.5,5589.3,7350.8,8236.8,8236.8,10433.,14654./

REFERENCES

1. E.V. Belousov and A.P. Motornenko, "Control of Electrical Parameters and Spectral Radiation in a Microwave Plasma", Opt. Spectros, **30**, 6, 539 (June 71).
2. R.G. Bosisio, C.F. Weissfloch, and M.R. Wertheimer, "The Large Volume Microwave Plasma Generator", J. Microwave Power, **7**, 4, 325 (1972).
3. J.E. Gerling and P. Jorgenson, Gerling-Moore Commercial Applicator.
4. First Quarterly Report of Contract F33615-75-C-1082, "Plasma Discharge Characteristics with Ionization by 2.45 GHz Microwaves", March (1975).
5. T.O. Perkins, "Hot-Switching High-Power cw", Microwave Journal, **59** (1975).
6. A. Galardini, Low Energy Electron Collision in Gases, Wiley (1972).
7. L.G.H. Huxley and R.W. Crompton, The Diffusion and Drift of Electrons in Gases, Wiley (1974).
8. R.D. Franklin, "Kinetic Model of the Oxygen-Iodine Transfer Laser", Laser Digest, AFWL-TR-74-241, p.280.
9. A.K. MacKnight and P.J. Modreski, "Chemical Production of Singlet Oxygen", Laser Digest, AFWL-TR-74-344, P.346.
10. L. Elias, E.A. Ogryzlo and H.I. Schiff, "Electrically Discharged O₂", Canad. J. Chem. **37**, 1680 (1959).
11. R.G. Derwent and B.A. Thrush, "Measurements on O₂ ¹Δ_g and O₂ ¹Σ_g⁺ in Discharge Flow Systems", Trans. Faraday Soc., **67**, 583 (1971).
12. E.A. Ogryzlo, "Why Liquid Oxygen is Blue", J. Chem. Education, **42**, 647 (1965).
13. R.J. Pirkle, J.R. Wisenfield, C.C. Davis, G.J. Wolga and R.W. McFarlane, "Production of Electronically Excited Iodine Atoms, I(²P_{1/2}), Following Injection of HI into Flow of Discharges Oxygen", IEEE J. of Quan. Elect., QE-11, 10 (Oct. 1975).
14. F. Kaufman and J. Kelso, "Reactions of Atomic Oxygen with Oxides of Nitrogen", 7th Combustion Symposium, P.53.
15. Fisher-Porter, Tri-Flat Variable-Area Flowmeter, Handbook 10A9010.
16. A Fisher-Porter Tri Flat Variable Area Flowmeter of the 1/16 series was used since the flow could be calculated as a function of fluid viscosity and density from the tube characteristics supplied by the manufacturer.

AD-A062 659

UNIVERSAL ENERGY SYSTEMS INC DAYTON OHIO
LARGE VOLUME PLASMA PRODUCTION BY 2.45GHZ MICROWAVES.(U)
DEC 77 R DARRAH

F/G 20/9

UNCLASSIFIED

AFAPL-TR-77-85

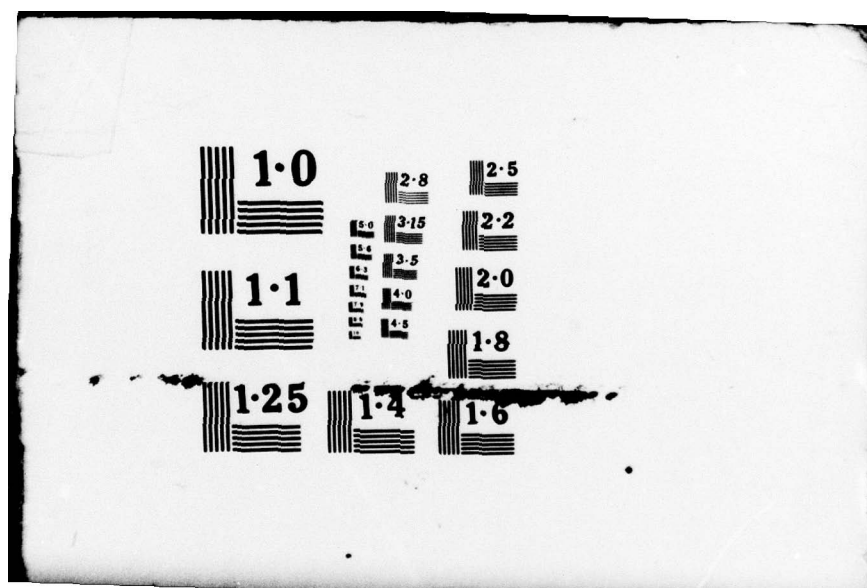
F33615-75-C-1082
NL

2 OF 2
ADA
062659



END
DATE
FILMED

3 -79
DDC



17. P. Gray and A.P. Yoffe, "The Reactivity and Structure of Nitrogen Dioxide", Chem. Rev., 55, 1069 (1955).
18. API Research Project 44, Selected Values of Properties of Hydrocarbons and Related Compounds, (Texas A&M University, College Station, Texas, 1956, 1960, 1962) Tables 18-1.
19. W.F. Giauque and J.D. Kemp, "The Entropies of Nitrogen Tetroxide and Nitrogen Dioxide. The Heat Capacity from 15°K to the Boiling Point. The Heat of Vaporization and Vapor Pressure. The Equilibria $N_2O_4 \rightleftharpoons 2NO_2 \rightleftharpoons 2NO + O_2$.", J. Chem. Phys., 6, 40 (1938).
20. M. Bodenstein and F. Boes, "Messungendes Gleichyewichts $N_2O_4 \rightleftharpoons 2NO_2$ ", Physik. Chem., (Lipzig) 100, 75 (1922).
21. F. Verhock and F. Daniels, "The Dissociation Constants of Nitrogen Tetroxide and of Nitrogen Trioxide", J. Am. Chem. Soc., 53, 1250 (1931).
22. M.E. Wourtzal, "Sur la Constante de Dissociation du Peroxyde d'Azote", Compt. Rend., 169, 1397 (1919).
23. I. Petker and D.M. Mason, "Viscosity of the $N_2O_4 \rightleftharpoons 2NO_2$ Gas System", J. Chem. Eng. Data, 9, 280 (1964).
24. A.K. Barua and T.K. Dastidar, "Force Constants of N_2O_4 and $2NO_2$ and the Viscosity of the Dissociating System $N_2O_4 \rightleftharpoons 2NO_2$ ", J. Chem. Phys., 43, 4140 (1969).
25. R.S. Browkaw and R.A. Svehla, "Viscosity and Thermal Conductivity of the $N_2O_4 \rightleftharpoons 2NO_2$ System", J. Chem. Phys., 44, 4643 (1966).
26. M. Ardon, Oxygen, W.A. Genjamin (1965).
27. A.M. Merns and A.J. Morris, "Production of Oxygen Atoms in Quartz and Polytetrafluoroethylene Discharge Tubes", Nature, 225 59 (1970).
28. R.A. McFarlane, "Microwave Discharge Atom Source for Chemical Lasers", Rev. Sci. Instrum., 46, 1063 (1975).
29. Laser purchased from Jodon, Engineering Assoc. Inc.
30. J.S. Whittier, M.L. Lindquist, A. Ching, G.E. Thornton, R. Hofland, Jr., "Dissociation Efficiency of Electron-Beam-Triggered Discharges for Initiating Atmospheric-Pressure $H_2 - F_2$ Lasers", J. of App. Phys., 47, 3542 (1976).
31. Fussion System Corporation, Bulletin RAD-2, S.
32. S.L. Bellinger, General Electric Review, 47, 31 (1944).
33. J.F. Waymouth, Electric Discharge Lamps, M.I.T. Press, (1971).